8010 J. Med. Chem. 2009, 52, 8010–8024
DOI: 10.1021/jm9013828

Journal of Medicinal Chemistry Article

# Discovery of 4-Morpholino-6-aryl-1*H*-pyrazolo[3,4-*d*]pyrimidines as Highly Potent and Selective ATP-Competitive Inhibitors of the Mammalian Target of Rapamycin (mTOR): Optimization of the 6-Aryl Substituent

Jeroen C. Verheijen,*[†] David J. Richard,[†] Kevin Curran,[†] Joshua Kaplan,[†] Mark Lefever,[†] Pawel Nowak,[†] David J. Malwitz,[†] Natasja Brooijmans,[†] Lourdes Toral-Barza,[‡] Wei-Guo Zhang,[‡] Judy Lucas,[‡] Irwin Hollander,[‡] Semiramis Ayral-Kaloustian,[†] Tarek S. Mansour,[†] Ker Yu,[‡] and Arie Zask[†]

[†]*Chemical Sciences and* [‡]*Oncology Research, Wyeth Research, 401 N. Middletown Road, Pearl River, New York 10965*

*Received July 23, 2009*

Design and synthesis of a series of 4-morpholino-6-aryl-1*H*-pyrazolo[3,4-*d*]pyrimidines as potent and selective inhibitors of the mammalian target of rapamycin (mTOR) are described. Optimization of the 6-aryl substituent led to the discovery of inhibitors carrying 6-ureidophenyl groups, the first reported active site inhibitors of mTOR with subnanomolar inhibitory concentrations. The data presented in this paper show that 6-arylureidophenyl substituents led to potent mixed inhibitors of mTOR and phosphatidylinositol 3-kinase α (PI3K-α), whereas 6-alkylureidophenyl appendages gave highly selective mTOR inhibitors. Combination of 6-alkylureidophenyl groups with 1-carbamoylpiperidine substitution resulted in compounds with subnanomolar $IC_{50}$ against mTOR and greater than 1000-fold selectivity over PI3K-α. In addition, structure based drug design resulted in the preparation of several 6-arylureidophenyl-1*H*-pyrazolo[3,4-*d*]pyrimidines, substituted in the 4-position of the arylureido moiety with water solubilizing groups. These compounds combined potent mTOR inhibition ($IC_{50}$ < 1 nM) with unprecedented activity in cellular proliferation assays ($IC_{50}$ < 1 nM).

## Introduction

Inhibition of components of the PI3K-Akt-mTOR[a] cascade, one of the most universally up-regulated signaling pathways in human cancers, is currently the focus of an intense effort directed at the identification of novel cancer drugs.[1−5] Rapamycin and its analogues ("rapalogues"), which inhibit the downstream component mTOR, have shown clinical efficacy in the treatment of cancer. Two rapalogues, temsirolimus and everolimus, were recently approved for the treatment of advanced, metastatic renal cell carcinoma. Rapamycin and its analogues inhibit only one of two functional complexes of mTOR (mTOR complex 1, mTORC1) while not affecting signaling through mTOR complex 2 (mTORC2).[6] mTORC2 phosphorylates Akt at serine-473, thereby contributing to full activation of Akt.[7] mTORC1 inhibition with rapalogues can lead to increased PI3K-Akt signaling, through removal of a negative feedback mechanism.[8] Increased Akt activity has antiapoptotic effects and may limit the anticancer efficacy of the rapalogues. In addition, recent reports suggest that rapalogues only partially inhibit mTORC1 activity.[9,10] Inhibition of mTOR at the active site by ATP-competitive inhibitors would be expected to decrease signaling through both mTORC1 and mTORC2 and could therefore give access to mTOR inhibitors with improved efficacy over the rapalogues.

Most of the reported ATP competitive inhibitors of mTOR also inhibit one or several related kinases, particularly PI3K.[11−13] PI3K is positioned upstream in the PI3K-Akt-mTOR signaling pathway and is a key mediator for signaling through the insulin receptor. Selective inhibition of mTOR without inhibiting PI3K could result in compounds with increased efficacy compared to the rapalogues and with increased tolerability compared to mixed PI3K/mTOR inhibitors. Very recently, several papers have appeared describing the biological activity of selective ATP competitive mTOR inhibitors.[14−18] In addition, our laboratory has revealed a series of 4-morpholino-6-aryl-1*H*-pyrazolo[3,4-*d*]pyrimidines (e.g., **1** and **2**, Figure 1) as ATP-competitive inhibitors of mTOR.[19−21]

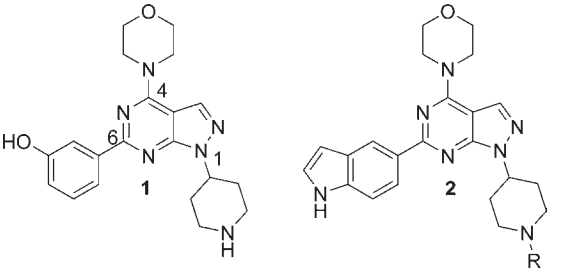


**Figure 1.** Pyrazolopyrimidine mTOR inhibitors.

*To whom correspondence should be addressed. Phone: +1 845 602 2800. Fax: +1 845 602 5561. E-mail: verheij@wyeth.com.

[a] Abbreviations: ACE-Cl, α-chloroethyl chloroformate; ATP, adenosine triphosphate; ATR, ataxia telangiectasia and Rad3 related; Delfia, dissociation-enhanced lanthanide fluorescent immunoassay; EDC, 1-ethyl-3-(3-dimethylaminopropyl)carbodiimide; HTS, high-throughput screening; mTOR, mammalian target of rapamycin; mTORC1, mammalian target of rapamycin complex 1; mTORC2, mammalian target of rapamycin complex 2; PI3K, phosphatidylinositol 3-kinase; PIKK, phosphatidylinositol 3-kinase related kinase; SAR, structure−activity relationships; SEM, standard error of the mean; TFA, trifluoroacetic acid.

 Published on Web 11/06/2009 

An mTOR Delfia HTS screen of our HTS collection followed by hit to lead optimization resulted in the discovery of **1**. Initial SAR studies revealed that the phenol in the 6-position of the pyrazolopyrimidine could be replaced with a 5-indolyl group, resulting in compounds such as **2** that are potent and selective inhibitors of mTOR.[20] We recently published preliminary data in a Letter describing the discovery of the 6-ureidophenyl group as an additional bioisostere for the phenol or indole groups. The resulting mTOR inhibitors combined excellent enzyme and cellular potency with high selectivity over PI3K.[19] We now follow up with an Article, presenting a comprehensive report of our modeling studies and lead optimization efforts leading to the discovery of 6-ureidophenyl containing mTOR inhibitors, as well as a detailed SAR study of this substituent and full experimental details. In addition, we present additional data highlighting the potency and selectivity of the resulting inhibitors at the enzymatic and cellular levels as well as in vivo.

**Scheme 1**[a]

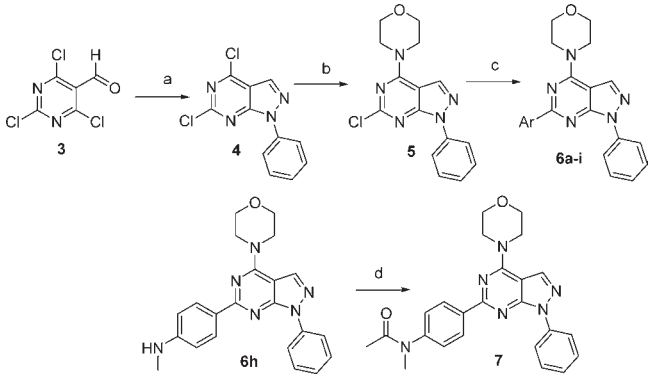


[a] Reagents and conditions: (a) phenylhydrazine; (b) morpholine, $NEt_3$; (c) $ArB(OR)_2$, $Pd(PPh_3)_4$; (d) $Ac_2O$.

## Chemistry

The synthesis of the 4-morpholino-6-aryl-1*H*-pyrazolo-[3,4-*d*]pyrimidines is depicted in the following schemes. As shown in Scheme 1, condensation of 2,4,6-trichloropyrimidine-5-carbaldehyde[22] (**3**) with commercially available phenylhydrazine provided 4,6-dichloropyrazolopyrimidine core **4**. Nucleophilic displacement of the 4-chloride with morpholine, to give 4-morpholinopyrazolopyrimidine **5**, was followed by Suzuki−Miyaura coupling to give target compounds **6**. In the case of *N*-methylaniline **6h**, the aniline was acylated to give amidoaryl **7**.

Following a similar procedure, compounds **13a**−**c**, containing an *N*-benzylpiperidine at the 1-position, could be prepared (Scheme 2). Thus, 1-benzyl-4-piperidone (**8**) was condensed with benzoic hydrazide, followed by debenzoylation of resulting **9** to give hydrazine **10**. Condensation of *N*-benzylpiperidinylhydrazine **10** with **3** was followed by the same sequence of reactions as described in Scheme 1, to give target compounds **13a**−**c**.

Pyrazolopyrimidines equipped with a ureidophenyl substituent in the 6-position were accessible as shown in Scheme 3. Reaction of 4-isocyanatophenyl boronate **14** with amines gave ureidophenyl boronate **15**. Suzuki−Miyaura coupling of boronates **15** with aryl chloride **12** gave access to **16**.

An alternative approach to ureidophenyl compounds is shown in Scheme 4. A 4-aminophenyl group was introduced in the 6-position as described above (**13a**). Activation of **13a** with triphosgene, followed by condensation with amines, provided **17**. The synthesis of compound **18**, an analogue of 4-ureidophenyl compounds **17** lacking one of the nitrogens, is presented in Scheme 4 as well. Thus, Suzuki−Miyaura

**Scheme 2**[a]

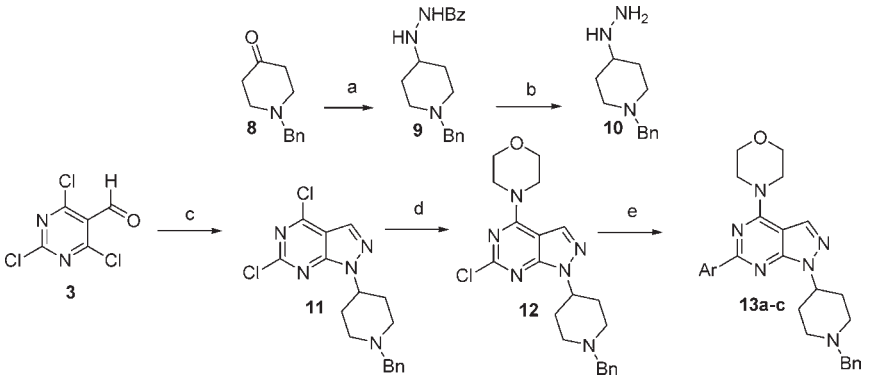


[a] Reagents and conditions: (a) benzoic hydrazide; (b) conc HCl, reflux; (c) **10**, $NEt_3$; (d) morpholine, $NEt_3$; (e) $ArB(OR)_2$, $Pd(PPh_3)_4$.

**Scheme 3**[a]

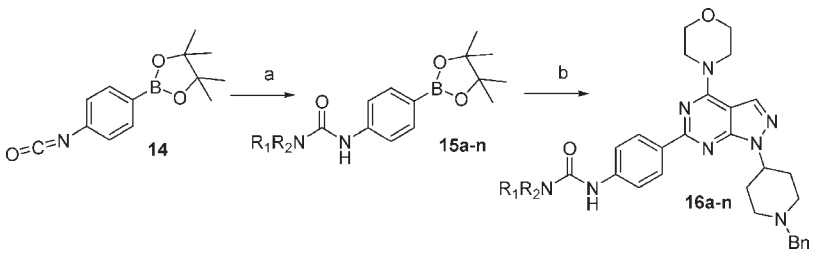


[a] Reagents and conditions: (a) $R_1R_2NH$; (b) **12**, $Pd(PPh_3)_4$.

**Scheme 4**[a]

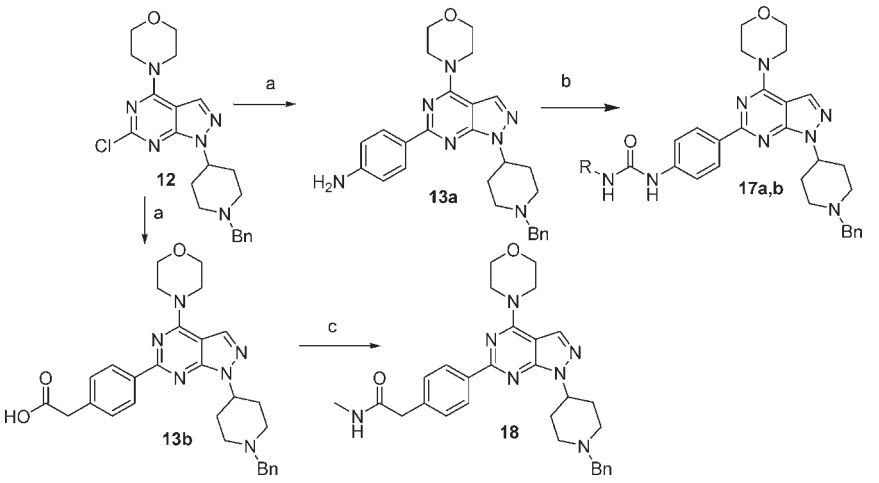


[a] Reagents and conditions: (a) $ArB(OR)_2$, $Pd(PPh_3)_4$; (b) (1) triphosgene, $NEt_3$; (2) $RNH_2$; (c) $MeNH_2$, EDC.

**Scheme 5**[a]

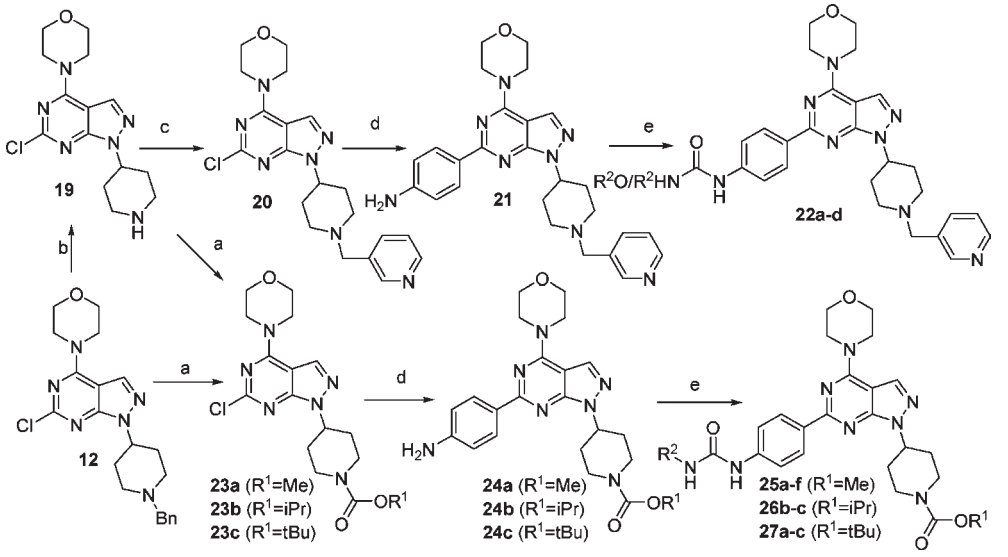


[a] Reagents and conditions: (a) $R^1OCOCl$; (b) ACE-Cl; (c) 3-pyridine carboxaldehyde, $NaHB(OAc)_3$; (d) $ArB(OR)_2$, $Pd(PPh_3)_4$; (e) (1) triphosgene, $NEt_3$, (2) $R^2OH/R^2NH_2$.

**Scheme 6**[a]

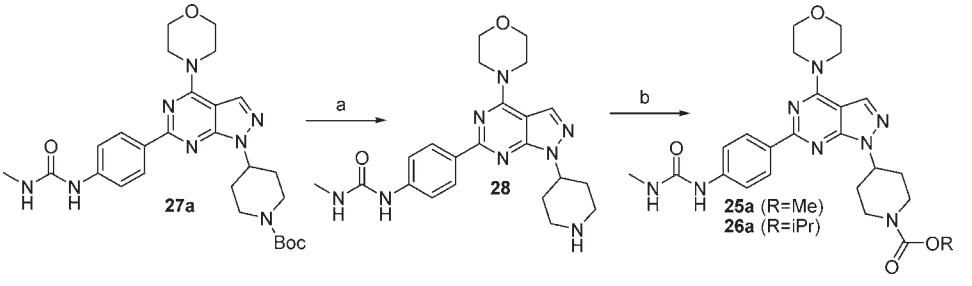


[a] Reagents and conditions: (a) TFA; (b) ROCOCl.

coupling with 2-(4-(4,4,5,5-tetramethyl-1,3,2-dioxaborolan-2-yl)phenyl)acetic acid gave carboxylate **13b**, which was condensed with methylamine under the agency of EDC to give **18**.

Scheme 5 outlines synthetic approaches to inhibitors containing various piperidine substituents. Replacement of the benzyl group in **12** with a methyl carbamate (**23a**) was effected by treatment with methylcarbamoyl chloride. Alternatively, carbamoyl piperidine compounds **23b**,**c** were accessible from free piperidine **19**, obtained after ACE chloride debenzylation of **12**. Piperidine **19** could also be converted into picolyl-functionalized **20** by reductive amination.

**Scheme 7**[a]

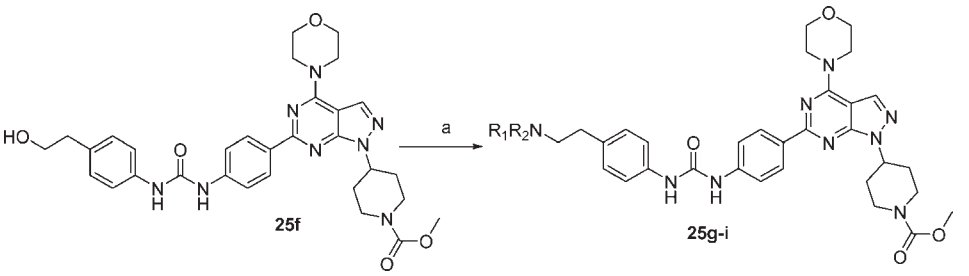


[a] Reagents and conditions: (a) $NEt_3$, TsCl, then $R_1R_2NH$.

Aryl chlorides **20** and **23** were subjected to Suzuki−Miyaura coupling conditions to give anilines **21** and **24**, respectively. Conversion of the aniline into a carbamoylphenyl or ureidophenyl group was effected as before, to give **22** and **25**−**27**.

An alternative approach to methylureido compounds **25a** and **26a** is presented in Scheme 6. Boc-protected analogue **27a** was converted into the free piperidine **28** by treatment with TFA. Treatment of **28** with chloroformates afforded carbamoylpiperidines **25a** and **26a**.

Further derivatization of hydroxyethylphenylureido compound **25f** is depicted in Scheme 7. Treatment of **25f** with *p*-toluenesulfonyl chloride followed by reaction with excess amine gave access to **25g**−**i**.

## Results and Discussion

Our initial efforts to discover bioisosteres of the 3-phenol group (cf. **1**) and 5-indole group (cf. **2**) focused on anilines and aminopyridines (Table 1). SAR studies were performed on the readily available 1-phenyl substituted pyrazolopyrimidine core. Comparison of indole analogue **6a** with aniline analogues **6b** and **6c** revealed that 3- or 4-anilino substitution in the pyrazolopyrimidine 6-position led to compounds with decreased mTOR inhibitory activity. However, introduction of a nitrogen into the ring, to give 2-aminopyridin-5-yl derivative **6d**, led to an 8-fold increase in potency compared to **6c**. Similar results were obtained for aminopyrimidines (Supporting Information, Table S1). In contrast, no such increase in potency was observed for regioisomeric aminopyridines (**6e** and **6f**). Molecular modeling provided an explanation for these findings. An mTOR homology model, based on the crystal structure of the related PI3K-$\gamma$ in complex with a compound from the pyrazolopyrimidine series,[19] was used to examine SAR. The catalytic domain of mTOR is 25% homologous to that of PI3K-$\gamma$, but the binding sites show significantly more conservation with 68% of the residues being identical. Modeling studies showed that the morpholinopyrimidines form a critical hydrogen bond to the backbone of the hinge region (Val2240) through the morpholine oxygen, while the indole NH of **6a** or the anilines of **6b**−**d** interact with Asp2195. In the case of aminopyridine **6d**, an additional hydrogen bond was observed between the catalytic lysine (Lys2187) and the pyridine nitrogen (Figure 2A). This interaction is not possible for regioisomers **6e** and **6f**. Finally, an additional interaction between Glu2190 and the exocyclic amine in **6d** was observed (Figure 2A).

It was clear from the data in Table 1 that combination of an H-bond donor (amino group) and H-bond acceptor (ring nitrogen) in the 6-substituent ("R" in Table 1) could give potent mTOR inhibitors. Interestingly, it was found

**Table 1.** Anilines and Aminopyridines

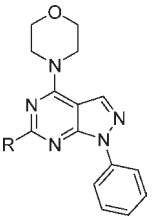

| *Cmpd.* | *R* | *mTOR* $IC_{50}$ *(nM)*[a] | *PI3K-α* $IC_{50}$ *(nM)*[a] | *Selectivity*[b] |
|---|---|---|---|---|
| **6a** |  | 27 +/- 8 | 231 +/- 44 | 9 |
| **6b** | 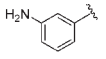 | 111 +/- 31 | 436 +/- 142 | 4 |
| **6c** | 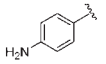 | 73 +/- 18 | 290 +/- <10 | 4 |
| **6d** | 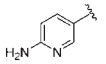 | 9.6 +/- 1.4 | 59 +/- 17 | 6 |
| **6e** | 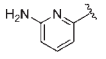 | 113 +/- 18 | 1,000 | 9 |
| **6f** | 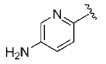 | 145 +/- 15 | 1,050 | 7 |
| **6g** | 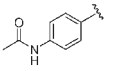 | 16+/-2.2 | 137+/-40 | 9 |
| **7** | 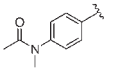 | 480+/-40 | 792+/-102 | 1.7 |
| **6i** | 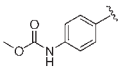 | 20 +/- 7.0 | 493 +/- 160 | 25 |

[a] Mean ± SEM. [b] Selectivity ($IC_{50}$ PI3K-α)/($IC_{50}$ mTOR).

that mTOR potency could be maintained when the H-bond donor (amino group) was combined with an exocyclic H-bond acceptor (carbonyl oxygen). Thus, acetamide **6g** possessed similar potency as aminopyridine **6d**. Methylation of the amide in **6g** to give **7** resulted in a 30-fold decrease in activity, highlighting the importance of the presence of an H-bond donor in that position. Molecular modeling of the binding mode of acetamide inhibitors confirmed the formation of H-bonds between the acetamide and Asp2195 and Lys2187

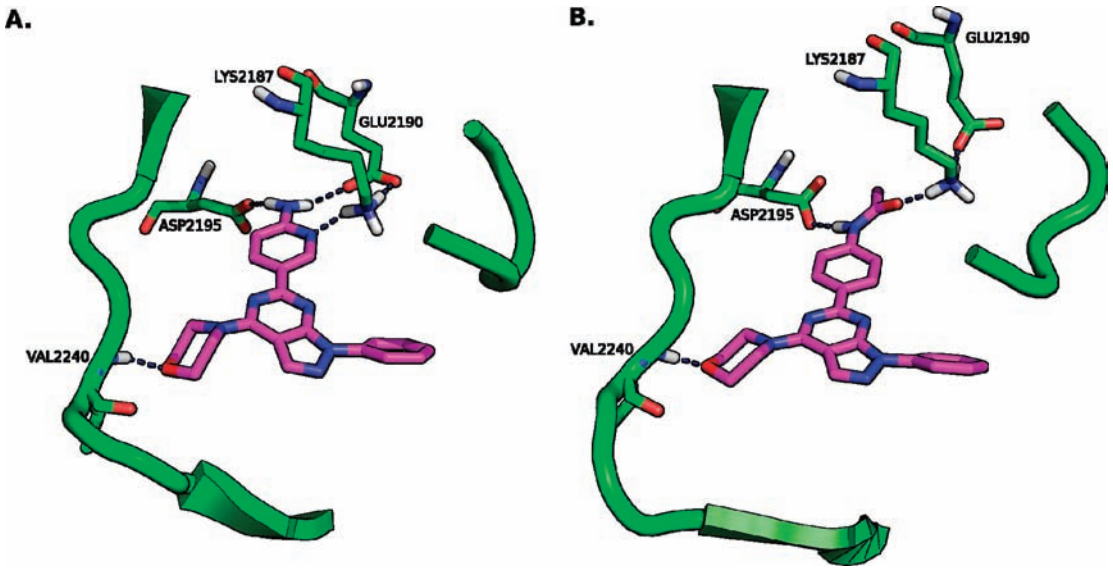


**Figure 2.** Close-up of binding interactions of inhibitors with mTOR homology model: (A) binding mode of aminopyridine **6d** showing hydrogen bonds (dashed lines) with Asp2195, Lys2187, and Glu2190 and the salt bridge between Lys2187 and Glu2190; (B) interactions of acetamide **6g** showing hydrogen bonds between the acetamide and Asp2195 and Lys2187 and the salt bridge between Lys2187 and Glu2190. Comparison of parts A and B highlights the observed concerted motion by Lys2187 and Glu2190 to maintain hydrogen bonding interactions with the inhibitors.

(Figure 2B). A comparison of the binding modes of aminopyridine **6d** (Figure 2A) and acetamide **6g** (Figure 2B) showed a concerted motion by the catalytic lysine (Lys2187) and its salt bridge partner Glu2190 to maintain hydrogen bonding interactions with the inhibitors.

Table 1 showed that the *m*-aniline possessed similar potency as the corresponding para-substituted inhibitor (compare **6b** and **6c**). The effect of meta- vs para-substitution was investigated in more detail. Small substituents (hydroxyl, amino) were equally tolerated in the meta and para positions, while larger amide substitutents were only tolerated at the para-position (Supporting Information, Table 2). Molecular modeling showed that incorporation of *m*-amidophenyl groups resulted in significant steric hindrance. Therefore, further efforts focused on the investigation of para-substituted aryl groups. Initially, the use of substituted amides for the introduction of water-solubilizing groups was explored. Although a variety of groups were tolerated, all substituted acetamides were only poorly selective over PI3K-α (Supporting Information, Table S3). In contrast, methyl carbamate **6i** possessed promising selectivity, although the potency ($IC_{50}$ = 10 $\mu$M) of **6i** in a prostate cancer cell line (LNCaP) proliferation assay required further optimization. When the corresponding 1-benzylpiperidinepyrazolopyrimidine (**13c**, Table 2) was prepared, it was found to possess greater potency in this cellular proliferation assay. Therefore, **13c** was selected as the starting point for further optimization.

SAR had shown that the 1-benzylpiperidine group could be replaced with a picolylpiperidine group.[19] This replacement was accompanied by a moderate increase in potency and selectivity (**22a**, Table 2). For further SAR studies, the benzylpiperidine and picolylpiperidine substituents at the pyrazolopyrimidine 1-position were used interchangeably. Larger alkyl carbamates (Et, Pr, $^i$Pr) resulted in 4- to 13-fold decreased potency (data not shown). Interestingly, the hydroxyethyl carbamate (**22b**) was 3-fold more potent than the corresponding methyl carbamate (**22a**). Molecular modeling provided an explanation for the high potency of hydroxyethyl carbamate **22b**. As shown in Figure 3A, the critical hydrogen bond to the backbone of the hinge region (Val2240) through the morpholine oxygen was maintained. The hydroxyethyl

**Table 2.** Carbamoyl and Ureidophenyl Analogues and Isosteres

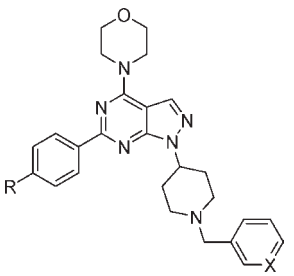

| *Cmpd.* | *R* | *X* | *mTOR* $IC_{50}$ *(nM)*[a] | *PI3K-α* $IC_{50}$ *(nM)*[a] | *Selectivity*[b] | *LNCaP cell* $IC_{50}$ *(nM)*[c] |
|---|---|---|---|---|---|---|
| **13c** |  | CH | 12 +/- 3.5 | 486 +/- 54 | 42 | 500 |
| **22a** | | N | 4.6 +/- 1.2 | 801 +/- 199 | 172 | 213 |
| **22b** | 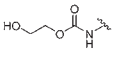 | N | 1.5 +/- 0.1 | 284 +/- 84 | 189 | 11 |
| **16a** |  | CH | 0.5 +/- 0.08 | 14 +/- 2.3 | 28 | 1.5 |
| **22c** | | N | 0.4 +/- 0.04 | 41 +/- 1.5 | 107 | 3.4 |
| **16b** |  | CH | 76 +/- 22 | 589 +/- 136 | 8 | 2,400 |
| **18** |  | CH | 170 +/- 50 | 4,058 | 24 | 9,300 |
| **16c** |  | CH | 16 +/- 0.3 | 317 +/- 10 | 20 | 500 |
| **22d** | | N | 23 | 1,005 +/- 47 | 44 | 500 |
| **16d** |  | CH | 84 +/- 14 | 1,935 +/- 74 | 23 | 3,500 |

[a] Mean ± SEM. [b] Selectivity ($IC_{50}$ PI3K-α)/($IC_{50}$ mTOR). [c] The average error for LNCaP $IC_{50}$ determinations was < 25%.

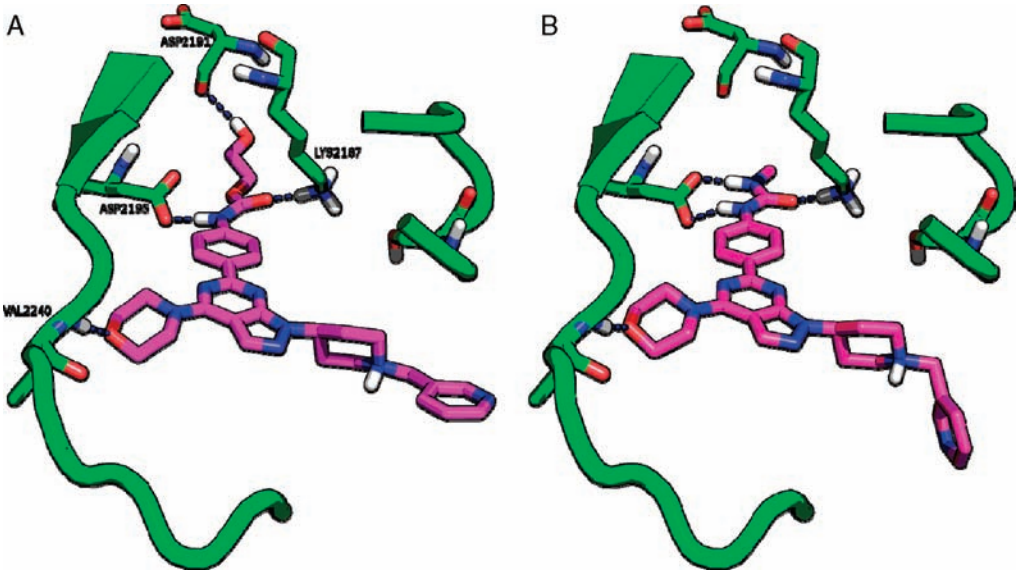


**Figure 3.** Close-up of binding interactions of inhibitors with mTOR homology model: (A) binding mode of hydroxyethyl carbamate **22b**; (B) interactions of methylurea **22c**. Hydrogen bonds are indicated by dashed blue lines. mTOR residue numbers are shown in part A.

carbamate of **22b** was able to form three additional hydrogen bonding interactions. The carbamate NH formed a hydrogen bond to the side chain of Asp2195, while the carbonyl interacted with the catalytic lysine (Lys2187). The hydroxyl group interacted with another aspartic acid further away from the ATP binding site (Asp2191) by forming a hydrogen bond to its backbone carbonyl group. A comparison to the binding modes of inhibitors containing an aminopyridine (cf. Figure 2A, one hydrogen bond to Asp2195 in addition to the hinge region interaction), 5-indole (one hydrogen bond to Asp2195 in addition to the hinge region interaction[20]) or 4-acetamide (cf. Figure 2B, two hydrogen bonds to Asp2195 and Lys2187 in addition to the hinge region interaction) reveals that the increased potency of the hydroxyethyl carbamate is likely caused by the formation of the additional hydrogen bond to Asp2191.

A further increase in enzyme inhibition was observed when the carbamoylphenyl group was replaced with a ureidophenyl group. Thus, methylureas **16a** and **22c** were 10- to 20-fold more potent than the corresponding methyl carbamates **13c** and **22a** and represent the first known subnanomolar inhibitors of mTOR. In addition, ureas **16a** and **22c** inhibited cellular proliferation at single digit nanomolar concentrations, a several-hundred-fold improvement over the corresponding carbamates **13c** and **22a**, respectively. Molecular modeling, based on an X-ray structure of a urea analogue bound to PI3K-$\gamma$ (PDB code 3IBE), again provided an explanation for the increased potency of the urea analogues. As shown in Figure 3B, in addition to the critical hinge region interaction, the urea of **22c** formed three hydrogen bonds. The carbonyl bound to the catalytic lysine (Lys2187) and both NH groups interacted with Asp2195.

In order to evaluate whether the potency in LNCaP cellular proliferation was predictive of activity in other cancer cell lines, several representative compounds were screened against a broad panel of tumor cells (Supporting Information, Table S4). The same trends as observed in LNCaP cells were evident in other cell lines as well. Ureas **16a** and **22c** were significantly more active than the corresponding carbamates **13c** and **22a** in all cell lines studied. Because mTOR mediates the PI3K-Akt signaling functions and PI3K/Akt hyperactive tumors more likely depend on mTOR for growth and survival, mTOR inhibitors may be more effective against a subset of tumors that express dysregulated PI3K/Akt signaling status. Thus, cell lines characterized by mutations that lead to hyperactive PI3K/Akt signaling (PTEN $-/-$ or PIK3CA) were especially sensitive to mTOR inhibitors (LNCaP, U87MG, PC3MM2, MDA361, and MCF7). Several cell lines not known to express dysregulation of PI3K/Akt signaling were somewhat less sensitive (MDA435, MDA231, DUI45, and HT29). The excellent potency of the urea-containing mTOR inhibitors is illustrated by the fact that even some of these less sensitive cell lines responded well to submicromolar concentrations of ATP-competitive mTOR inhibitors.

On the basis of this excellent activity, analogues of **16a** and **22c** were explored in more detail. First, consistent with the proposed binding mode, the importance of the presence of both urea NH groups as potential hydrogen bond donors was confirmed by compounds **16b** and **18**. Thus, 1-N-methylation (**16b**) resulted in a greater than 100-fold decrease in potency. Similarly, removal of the urea 3-NH (**18**) led to a greater than 300-fold decrease in activity. Modifying the electronics of the ureido NH by conversion to a 1-methoxyurea (**16c**, **22d**) or a hydrazinecarboxamide group (**16d**) also led to significantly decreased potency.

Additional analogues and isosteres of the urea group were explored (e.g., thiourea, cyanoguanidine), but in all cases their potency against mTOR was inferior to that of the corresponding urea compounds (Supporting Information, Table S5). Substitution on the ureidophenyl group was explored in more detail (Table 3). Alkylureas (**16a**, **16f**, and **16g**) were more potent than unsubstituted urea **16e**. Ethyl- and 2-fluoroethylureas **16f** and **16g** possessed similar enzyme potency and somewhat decreased cellular potency compared to methylurea **16a**, but their selectivity was much higher. Branched urea **16h** was not as potent as **16a**. The increased activity of the smaller cyclopropyl analogue (**17a**) compared to the isopropyl compound (**16h**) suggests that this was due to steric hindrance. With the exception of hydroxyethylurea **16i**, attempts to introduce water solubilizing ureas (**16j**–**l**) resulted in decreased potency and selectivity. Arylureido compounds (**16m**, **16n**, **17b**) led to highly potent mTOR inhibitors that

**Table 3.** Ureidophenyl SAR

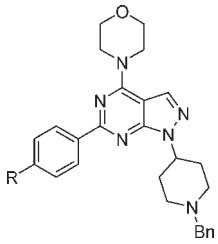

| *Cmpd.* | *R* | *mTOR* $IC_{50}$ *(nM)*[a] | *PI3K-α* $IC_{50}$ *(nM)*[a] | *Selectivity*[b] | *LNCaP cell* $IC_{50}$ *(nM)*[c] |
|---|---|---|---|---|---|
| **16a** |  | 0.5 +/- 0.08 | 14 +/- 2.3 | 28 | 1.5 |
| **16e** |  | 2.7 +/- 0.4 | 83 +/- 12 | 31 | 32 |
| **16f** |  | 0.8 +/- 0.3 | 257 +/- 22 | 321 | 30 |
| **16g** | 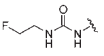 | 1.4 +/- 0.1 | 234 +/- 44 | 167 | 95 |
| **16h** |  | 4.8 +/- 0.6 | 270 +/- 52 | 56 | 560 |
| **17a** |  | 2.6 +/- 0.7 | 323 +/- 7.0 | 124 | 50 |
| **16i** | 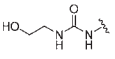 | 0.3 +/- 0.03 | 86 +/- 19 | 282 | 26 |
| **16j** | 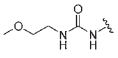 | 23 +/- 4.8 | 401 +/- 28 | 17 | 800 |
| **16k** | 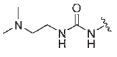 | 65 +/- 2.0 | 29 +/- 11 | 0.4 | 95 |
| **16l** | 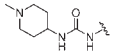 | 125 | 708 +/- 147 | 5.7 | 1,100 |
| **16m** | 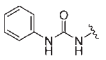 | 2.4 +/- 0.3 | 16.5 +/- 3.5 | 6.9 | 200 |
| **16n** | 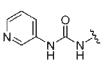 | 0.8 +/- 0.1 | 55 +/- 6.0 | 69 | 180 |
| **17b** | 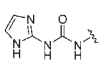 | 0.7 +/- 0.2 | 30 +/- 7.0 | 43 | 1,000 |

[a] Mean ± SEM. [b] Selectivity ($IC_{50}$ PI3K-α)/($IC_{50}$ mTOR). [c] The average error for LNCaP $IC_{50}$ determinations was < 25%.

were slightly less selective over PI3K-α than short chain alkylureido compounds.

Compounds incorporating benzylpiperidines and picolylpiperidines at the 1-position generally possessed poor microsomal stability. For instance, picolylpiperidine **22c** was degraded in nude mouse microsomes with a half-life of 12 min, whereas the benzylpiperidines were even more rapidly metabolized. We have previously reported that carbamoylpiperidines in the 1-position can improve microsomal stability.[19] Combination of carbamoylpiperidines in the 1-position with ureidophenyl groups in the 6-position led to several compounds that combined highly potent inhibition of mTOR ($IC_{50}$ < 1 nM) with excellent selectivity over PI3K-α (> 1000-fold) and potent (low double-digit nanomolar) inhibition of cellular proliferation (Table 4). In order to explore whether this unprecedented selectivity was specific to the α-isoform of PI3K, the $IC_{50}$ values against PI3K-γ and another PIKK, ATR, were also determined. In all cases, selectivity over PI3K-γ and ATR was greater than over PI3K-α. In this respect, incorporation of isopropylcarbamoylpiperidines in the 1-position led to the most selective compounds. It was also evident that 2-fluoroethylureidophenyl and cyclopropylureidophenyl groups in the 6-position led to more selective mTOR inhibitors compared to methylureidophenyl groups.

The microsomal stability data revealed that the carbamoylpiperidines were significantly more stable than the benzyl- and picolylpiperidines. We also explored the potential for drug−drug interaction by examining inhibition of various cytochrome P450 isoforms. At 3 μM, approximately 5000-fold the mTOR $IC_{50}$, none of the carbamoylpiperidines inhibited CYP 2D6 more than 20%. The methylcarbamoylpiperidines showed no inhibition of CYP 2C9 (< 20%) and low inhibition of CYP 3A4 (< 40%). The more lipophilic isopropyl- and *tert*-butylcarbamoylpiperidines showed slightly increased inhibition of the last two isoforms (3A4, 23−70%; 2C9, 40−75% at 3 μM).

In order to further evaluate the selectivity of the urea-containing inhibitors, representative compounds were assayed against a broad panel of 26 kinases (Supporting Information, Table S6). Although the methyl carbamate **22a** displayed excellent selectivity over all non-PIKKs in the panel (> 3500-fold), the selectivity of urea inhibitors **22c** and **27a** was particularly impressive (> 100000-fold over all non-PIKKs in the panel). The latter observation could be explained by the unique interaction of the urea with the active site in mTOR and PI3K involving the formation of three hydrogen bonds. Kinases outside the PIKK family do not have the ability to form these same interactions. Methylurea **22c** was also highly selective over the β- and δ-isoforms of PI3K ($IC_{50}$ of 141 and 64 nM, respectively). Finally, the less selective methyl carbamate (**22a**) was screened in a panel of 59 kinases by Invitrogen. At 1 μM, the only kinase showing > 20% inhibition was RAF1 (cRAF, 31%), providing further evidence that this class of inhibitors is highly selective for mTOR and the PIKKs.

Having identified potent and selective inhibitors of mTOR, we were interested in exploring how these inhibitors compared to previously disclosed ATP-competitive mTOR inhibitors. To this end, **31** (Ku-0063794),[16,18] one of the most potent and selective inhibitors reported to date, was synthesized according to literature procedures. Under our assay conditions, **31** inhibited mTOR with an $IC_{50}$ of 2.5 nM, was ~200-fold selective over PI3K-α, and inhibited LNCaP cellular proliferation with an $IC_{50}$ of 500 nM. Comparison of these values to the compounds in Table 4 revealed that the pyrazolopyrimidines were significantly more potent inhibitors of mTOR and cellular proliferation than **31**. In addition, several pyrazolopyrimidines were significantly more selective over PI3K (**25b**,**c**, **26a**−**c**, **27b**,**c**) than the selective inhibitor **31**.

mTOR inhibition was also explored at the cellular level in U87MG tumor cells (Figure 4). The ATP competitive inhibitors potently inhibited phosphorylation of the mTORC1 substrate P-S6K (T389) (< 100 nM). Slightly higher concentrations were required for inhibition of another mTORC1 substrate (P-4EBP1 (T70)) and the mTORC2 substrate P-Akt (S473) (< 300 nM). These values correlate well with the observed $IC_{50}$ values for inhibition of cellular proliferation

**Table 4.** Highly Selective mTOR Inhibitors Combining Alkylureidophenyl Substitution in the 6-Position with Carbamoylpiperdine Substitution in the 1-Position

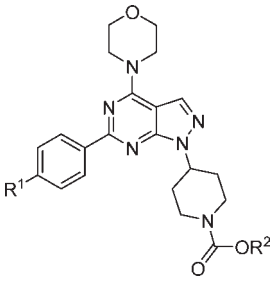

| Cmpd | $R^1$ | $R^2$ | mTOR $IC_{50}$ (nM)[a] | PI3K-α $IC_{50}$ (nM)[a] | Sel.[b] | PI3K-γ $IC_{50}$ (nM)[c] | ATR $IC_{50}$ (nM)[c] | LNCaP cell $IC_{50}$ (nM)[d] | N. Mouse micr.[e] |
|---|---|---|---|---|---|---|---|---|---|
| **25a** | | Me | 0.5 +/- 0.08 | 100 +/- 17 | 220 | 148 | 4,800 | 31 | >30 |
| **26a** |  | iPr | 0.2 +/- 0.02 | 189 +/- 16 | 857 | 1,431 | 7,700 | 28 | 19 |
| **27a** | | tBu | 0.7 +/- 0.2 | 80 +/- 7.0 | 117 | 409 | 11,700 | 27 | >30 |
| **25b** | | Me | 0.6 +/- 0.04 | 505 +/- 224 | 835 | 1,697 | 41,500 | 53 | >30 |
| **26b** | 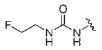 | iPr | 0.3 +/- 0.01 | 1,207 | 3,772 | 3,765 | >50,000 | 40 | 24 |
| **27b** | | tBu | 0.5 +/- 0.07 | 786 +/- 230 | 1,587 | 2,526 | >50,000 | 110 | 27 |
| **25c** | | Me | 0.5 +/- 0.04 | 661 +/- 157 | 1,468 | 1,772 | 26,200 | 42 | >30 |
| **26c** |  | iPr | 0.5 +/- 0.01 | 1,782 | 3,637 | 3,554 | >50,000 | 50 | 24 |
| **27c** | | tBu | 0.6 +/- 0.1 | 898 | 1,403 | 1,290 | >50,000 | 160 | 25 |

[a] Mean ± SEM. [b] Selectivity ($IC_{50}$ PI3K-α)/($IC_{50}$ mTOR). [c] The average error for PI3K-γ and ATR $IC_{50}$ determinations was < 50%. [d] The average error for LNCaP $IC_{50}$ determinations was < 25%. [e] Microsomal stability ($t_{1/2}$, min.).

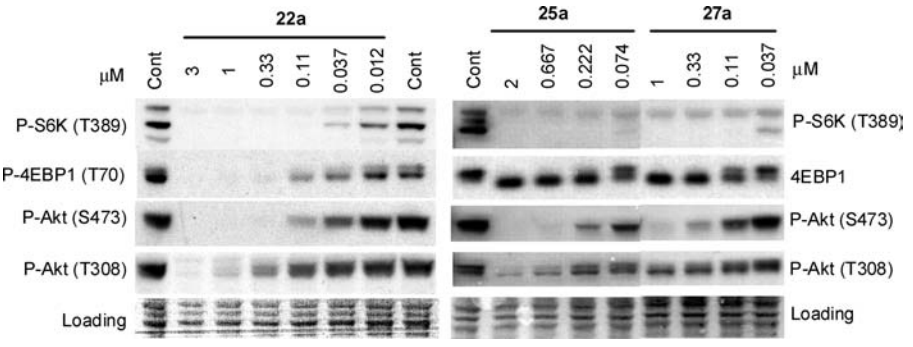


**Figure 4.** Inhibition of mTOR signaling after treatment with mTOR kinase inhibitors. U87MG cells were treated in growth medium for 6 h with the indicated concentrations of **22a**, **25a**, and **27a**. Total cell lysates were prepared and subjected to immunoblotting with antibodies against P-S6K, P-4EBP1 (T70), 4EBP1, P-Akt (S473), P-Akt (T308). The blots were also stained for Ponceau-S, a dye for total protein, for sample loading control.

in this cell line (12−120 nM). Selectivity over PI3K was evident at the cellular level as well. Thus, whereas the mTORC1 and mTORC 2 biomarkers were completely inhibited below 300 nM, inhibition of the PI3K/PDK1 biomarker P-Akt (T308) required significantly higher levels.

To confirm that the selectivity observed in vitro translated to selective inhibition of mTORC1 and mTORC2 in vivo, PC3MM tumor bearing nude mice were dosed intravenously with 50 mg/kg of compounds **25a** and **27a**. One hour after dosing, complete suppression of the mTORC1 substrate S6K was observed in the tumors (Figure 5), resulting in a significant decrease in phosphorylation of its target (P-S6). Likewise, near complete suppression of mTORC2 activity was observed (P-Akt (S473)). In sharp contrast, only negligible inhibition of phosphorylation of the PI3K/PDK1 biomarker (P-Akt (T308)) was observed, illustrating the fact that these compounds behave as selective inhibitors of mTOR in vivo.

Water solubilizing groups are often incorporated in kinase inhibitors to improve their physicochemical properties. It has already been shown (Table 3) that incorporation of water solubilizing alkylureidophenyl groups at the 6-position led to decreased potency and selectivity. Similar results were observed when water solubilizing groups were introduced at the

1-position of the pyrazolopyrimidines (data not shown). A careful examination of the three-dimensional structure of phenylureidophenyl inhibitor **25d** (Table 5), docked in an mTOR homology model based on a human PI3K-$\gamma$ crystal structure (PDB code 3IBE), indicated that the 4-position of the phenyl ring was exposed to solvent (Figure 6). The latter observation suggested that water solubilizing groups might be introduced in the para-position of arylureidophenyl groups at the 6-position of the pyrazolopyrimidines. Indeed, as shown in Table 5, introduction of an *N*-methylpiperazine in the para-position of the phenylureido moiety led to a compound (**25e**) that was as potent as the unsubstituted phenylureido analogue (**25d**). Selectivity over PI3K-α was also not affected by introduction of the water solubilizing group. A variety of other polar groups could also be incorporated in the same position while maintaining mTOR inhibitory activity and selectivity over PI3K-α (**25f**−**i**). In all cases, the selectivity over PI3K-$\gamma$ and ATR was even greater, with ATR selectivity in all cases > 20000-fold. Moreover, the cellular potency was greatly increased by the introduction of water solubilizing groups, resulting in the first known mTOR inhibitors with subnanomolar potency in cellular proliferation assays. These observations are in sharp contrast to the pronounced decrease in activity that was observed for direct linkage of polar groups on an alkyl chain to the ureidophenyl moiety (Table 3). The *N*-methylpiperazinophenylurea analogue **25e** displayed excellent stability in nude mouse microsomes. Although aminoethylphenylureas (**25g**−**i**) possessed poor to moderate stability in this assay, all compounds containing a basic amine had excellent stability in human microsomes (**25e**,**g**−**i**). In contrast, the hydroxyethyl substituent led to poor stability in human and nude mouse microsomes (**25f**). While unsubstituted phenylurea **25d** significantly inhibited CYP 3A4 (87% at 3 $\mu$M), analogues **25e**, **25g**, and **25h** showed no inhibition of CYP isoforms ( < 10% inhibition at 3 $\mu$M). Moderate inhibition of CYP 3A4 was observed for hydroxyethylurea **25f** and morpholinophenylurea **25i** (50% and 28%, respectively). Interestingly, the introduction of the morpholine moiety led to increased inhibition of CYP2C9 (58% for **25i** at 3 $\mu$M).

Comparison of the data in Tables 4 and 5 revealed that the tools are now available to design highly potent inhibitors (enzyme $IC_{50}$ < 1 nM, cellular $IC_{50}$ < 50 nM) with excellent selectivity ( > 1000-fold over PI3K-α) or to design compounds with further increased cellular potency ($IC_{50}$ < 1nM) but decreased selectivity (~50-fold over PI3K-α). It is currently not clear what levels of selectivity are required for optimal

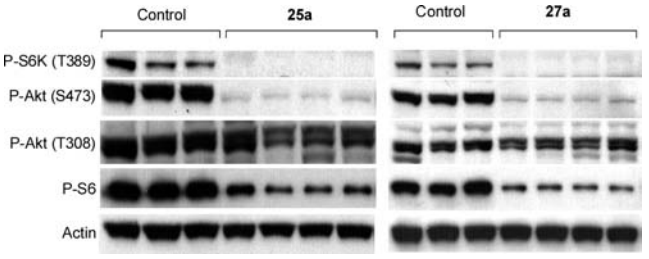


**Figure 5.** Inhibition of mTOR signaling in vivo following a single dose of mTOR kinase inhibitors. Nude mice bearing sc PC3MM2 tumors were injected iv with vehicle or 50 mg/kg test article. Tumor lysates were prepared 1 h after injection and were immunoblotted with antibodies against P-S6K (T389), P-Akt (S473), P-Akt (T308), P-S6, and $\beta$-actin.

**Table 5.** Water Solubilizing Groups in 4-Position of Arylureidophenyl Substituents

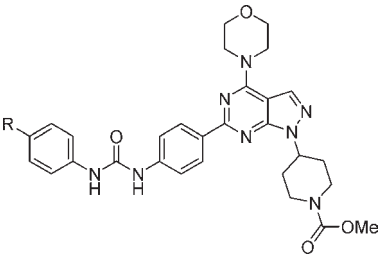


| *Cmpd.* | *R* | *mTOR* $IC_{50}$ *(nM)*[a] | *PI3K-α* $IC_{50}$ *(nM)*[a] | *Sel.*[b] | *LNCaP cell* $IC_{50}$ *(nM)*[c] | *N. Mouse micr.*[d] | *Human micr.*[d] |
|---|---|---|---|---|---|---|---|
| **25d** |  | 0.3 +/- 0.06 | 17 +/- 1.5 | 55 | 27 | 21 | - |
| **25e** |  | 0.3 +/- 0.02 | 15 +/- 1.5 | 48 | <1 | >30 | >30 |
| **25f** |  | 0.1 +/- 0.005 | 10 +/- <1 | 100 | <1 | 7 | <1 |
| **25g** | 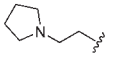 | 0.7 +/- 0.2 | 34 +/- 15 | 48 | <1 | 8 | >30 |
| **25h** | 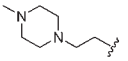 | 0.8 +/- 0.08 | 21 +/- 3.5 | 26 | 1.4 | 21 | >30 |
| **25i** | 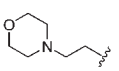 | 0.6 +/- 0.01 | 41 +/- 14 | 68 | 5.0 | 12 | >30 |

[a] Mean ± SEM. [b] Selectivity ($IC_{50}$ PI3K-α)/($IC_{50}$ mTOR). [c] The average error for LNCaP $IC_{50}$ determinations was < 25%. [d] Microsomal stability ($t_{1/2}$, min.).

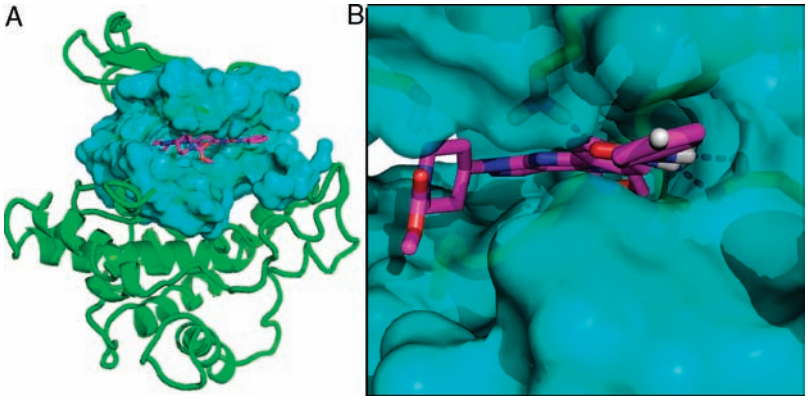


**Figure 6.** Surface representations of the mTOR binding site highlighting the tight fit of inhibitors as exemplified by phenylureidophenyl **25d**. (A) Overview of the mTOR catalytic domain in cartoon representation and the binding site in surface representation. **25d** is sandwiched between the N-lobe and C-lobe of the catalytic domain. (B) Close-up view of **25d** rotated 90° compared to part A. The hydrogen atom in the 4-position of the terminal phenyl ring is shown to illustrate the directionality toward solvent from this position. Hydrogen bonds between the urea and Lys2187 and Asp2195 are maintained (cf. Figure 3B) and are shown by dashed lines.

clinical efficacy. On one hand, highly selective mTOR inhibitors (i.e., the rapalogues) have proven efficacious in the treatment of certain cancers. On the other hand, ATP competitive mixed inhibitors of mTOR and PI3K are currently advancing through clinical development. With the tools now at our disposal, we expect to be able to further advance our understanding of the biology of inhibition of the mTOR pathway and to elucidate in more detail the role that PI3K and mTOR play in determining efficacy and side effects.

## Conclusions

The 4-ureidophenyl group was identified as an essential substituent in the 6-position of pyrazolopyrimidine inhibitors of mTOR, leading to highly potent (subnanomolar) inhibitors. Moreover, several highly selective compounds (>1000-fold selective over PI3K-α) with good cellular potency ($IC_{50}$ = 20−50 nM) were reported. In addition, we have presented compounds with good selectivity (50- to 100-fold over PI3K-α) that are extremely potent in cellular proliferation assays ($IC_{50}$ < 1 nM). The pharmacological tools now at our disposal should prove valuable in advancing our understanding of the role of this fascinating signaling pathway in cancer biology.

## Experimental Section

**Materials and Methods.** All solvents were HPLC grade, and all other chemicals were analytical reagent or equivalent. All chemicals were used as received. $^1$H NMR spectra were determined with a Bruker DRX400 spectrometer at 400 MHz or a NT-300 WB spectrometer at 300 MHz. Chemical shifts ($\delta$) are expressed in parts per million relative to the internal standard tetramethylsilane. Electrospray mass spectra were recorded in positive mode on a Micromass Platform spectrometer. High-resolution mass spectra (HRMS) were obtained on a Finnigan MAT-90 spectrometer or a Bruker 9.4T FTMS spectrometer. Chromatographic purifications were by flash chromatography using Baker 40 $\mu$m silica gel. Semipreparative reverse-phase high-pressure liquid chromtography (RP-HPLC) was performed using a Gilson Preparatory HPLC. The sample was dissolved in DMSO, applied on a Waters Atlantis Prep T3 OBD column (30 mm × 150 mm, 5 $\mu$m), and eluted at 30 mL/min with a 20 min gradient (from 5% B to 100% B), where solvent A is water (0.05% TFA buffer) and solvent B is acetonitrile (0.05% TFA buffer). An alternative solvent system consisted of solvent A being water (0.1% $NH_4OH$ buffer) and solvent B being acetonitrile (0.1% $NH_4OH$ buffer). The purity of tested compounds was determined by HPLC and was ≥95% except as noted.

**mTOR, PI3K, and ATR Assays.** A Flag-tagged truncated human TOR (Flag-TOR(3.5), amino acids 1360−2549) was expressed in HEK293 cells and affinity purified. The routine inhibitor assays were performed in 96-well plates for 2 h at room temperature in 25 $\mu$L containing 6 nM Flag-TOR(3.5) (estimated 5−10% purity), 1 $\mu$M His6-S6K, and 100 uM ATP. The assays were performed and detected by DELFIA employing the Eu-phospho-p70S6K T389 antibody.[23] The PI3K assays were performed as described previously,[24] using enzymes from Upstate Biotech (now Millipore). ATR kinase activity was evaluated using a DELFIA assay format.

**LNCap Tumor Cell Growth Assay.**[25] The LNCap cell line was obtained from the American Type Culture Collection (ATCC) and was maintained in a 37 °C incubator with 5% $CO_2$, and was cultured using standard cell culture methods. Cells were plated in 96-well culture plates at 1000−3000 cells per well for 24 h, treated with DMSO or various doses of mTOR inhibitors. Viable cell densities were determined 3 days later by MTS assay employing an assay kit (CellTiter 96 $AQ_{ueous}$, catalog no. G5421, Promega) following the kit assay protocol. The effect of each treatment was calculated as percent of control growth relative to the DMSO-treated cells grown in the same culture plate. Inhibitor dose−response curves were plotted for determination of $IC_{50}$ values.

**Determination of mTOR Inhibition in U87 Cells.**[21] Total cell lysates were prepared using NuPAGE-LDS sample buffer (Invitrogen), quantified by RCDC protein assay (Bio-Rad), and immunoblotted using NuPAGE electrophoresis system (Invitrogen). The following antibodies were obtained from Cell Signaling Technology: P-Akt (S473), P-Akt (T308), P-S6K1 (T389), P-4EBP1 (T70), 4EBP1.

**Inhibition of mTOR in Nude Mouse Xenograft Tumors.** U87MG tumors (400 $mm^3$) were grown subcutaneously in Balb/c nu/nu female mice, and vehicle or compound was dosed by a single intravenous injection (iv). Tumor lysates were prepared and immunoblotted.[26]

**Microsomal Stability.** Microsomal stability was determined as described previously.[27]

**mTOR Homology Model.** An mTOR homology model was built based on an in-house PI3K-$\gamma$ crystal structure in complex with a compound from the pyrazolopyrimidine series.[19] PRIME 1.5 [Prime, version 1.5, Schrödinger, LLC, New York, NY, 2005] was used to build the initial model, which was further optimized using EMBRACE (MacroModel, version 9.1, Schrödinger, LLC, New York, NY, 2005) minimizations in complex with the cocrystallized ligand.

Subsequent docking studies were performed using Glide 4.0 (Glide, version 4.0, Schrödinger, LLC, New York, NY, 2005) and 4.5 (Glide, version 4.5, Schrödinger, LLC, New York, NY, 2005) with the Single Precision (SP) scoring function. A hydrogen bonding constraint to valine-2240 of the hinge region was used during the docking.

**2,4,6-Trichloropyrimidine-5-carbaldehyde (3).** To a solution of $POCl_3$ (200 mL) in DMF (42 mL) cooled to 0 °C was slowly added barbituric acid (30 g) over 1.5 h. The mixture was then heated to reflux for 16 h and then evaporated (the distillate was carefully decomposed by slowly pouring into a stirred ice methanol slush). The remainder was cooled to 0 °C and added very slowly to a solution of ice−water upon which a beige solid formed. The solid was filtered, dissolved in DCM, washed with water, washed with a saturated $NaHCO_3$ solution, dried ($MgSO_4$), and concentrated in vacuo to give white crystals (24 g). $^1$H NMR ($CDCl_3$): $\delta$ 10.42 (1H, s).

**6-Chloro-4-morpholin-4-yl-1-phenyl-1*H*-pyrazolo[3,4-*d*]pyrimidine (5).** To a solution of 5.0 g (23.6 mmol) of 2,4,6-trichloropyrimidine-5-carbaldehyde (**3**) in ethanol, cooled at −78 °C, was added triethylamine (10 mL). Phenylhydrazine (2.32 mL, 23.6 mmol) was added slowly, and the mixture was allowed to warm to ambient temperature. The mixture was cooled to −78 °C again, and morpholine (2.2 mL, 25 mmol) was added. The mixture was allowed to warm to room temperature, and the resulting solids were collected by filtration, washed with ethanol, and dried to give 5.6 g (17.7 mmol) of the title compound. HRMS: $m/z$ 316.0960 ($[M + H]^+$). For $[M + H]^+$ mass error = 0.1 mDa or 0.16 ppm. $^1$H NMR (DMSO-$d_6$): $\delta$ 8.62 (1H, s), 8.03 (2H, d, $J$ = 8.8 Hz), 7.58 (2H, t, $J$ = 7.8 Hz), 7.40 (1H, t, $J$ = 7.4 Hz), 3.95 (4H, t, $J$ = 4.8 Hz), 3.78 (4H, t, $J$ = 4.8 Hz).

**General Procedure for Suzuki−Miyaura Coupling of 6-Chloro-4-morpholin-4-yl-1-phenyl-1*H*-pyrazolo[3,4-*d*]pyrimidine (5).** 6-Chloro-4-morpholin-4-yl-1-phenyl-1*H*-pyrazolo[3,4-*d*]pyrimidine (**5**, 38 mg, 0.12 mmol) was placed in a 0.5−2 mL microwave vial. Then 0.2 mmol of a boronic acid or boronate pinacol ester was added, followed by addition of 2 mL of dimethoxyethane and 0.25 mL of a 2 M aqueous solution of sodium carbonate. Tetrakis-(triphenylphosphine)palladium(0) (14 mg, 0.1 equiv) was added, and the mixture was heated for 10−30 min at 185 °C under microwave irradiation. The mixture was concentrated, dissolved in DMSO, filtered, and purified by reversed phase HPLC (TFA buffers) to give the target compound.

The following compounds were made according to the general procedure.

**4-(4-Morpholin-4-yl-1-phenyl-1*H*-pyrazolo[3,4-*d*]pyrimidin-6-yl)aniline (6c).** Yield: 31 mg (0.086 $\mu$mol, 71%). LCMS: 91% pure, $t_R$ = 2.33 min, $m/z$ 373.2 ($[M + H]^+$). HRMS: $m/z$ 373.177 99 ($[M + H]^+$). For $[M + H]^+$ mass error = 0.85 mDa or 2.29 ppm. $^1$H NMR (DMSO-$d_6$): $\delta$ 8.50 (1H, s), 8.32 (2H, d, $J$ = 8.4 Hz), 8.16 (2H, d, $J$ = 8.8 Hz), 7.60 (2H, t, $J$ = 8.0 Hz), 7.36 (1H, t, $J$ = 7.4 Hz), 6.64 (2H, d, $J$ = 8.8 Hz), 5.64 (2H, bs), 4.02 (4H, t, $J$ = 4.2 Hz), 3.81 (4H, t, $J$ = 4.4 Hz).

**5-(4-Morpholino-1-phenyl-1*H*-pyrazolo[3,4-*d*]pyrimidin-6-yl)-pyridin-2-amine (6d).** Yield: 21 mg (0.056 $\mu$mol, 47%). LCMS: 100% pure, $t_R$ = 1.94 min, $m/z$ 374.2 ($[M + H]^+$).

***N*-[4-(4-Morpholin-4-yl-1-phenyl-1*H*-pyrazolo[3,4-*d*]pyrimidin-6- yl)phenyl]acetamide (6g).** Yield: 14 mg (0.033 $\mu$mol, 28%). LCMS: 96.5% pure, $t_R$ = 2.41 min, $m/z$ 415.2 ($[M + H]^+$).

***N*-Methyl-4-(4-morpholino-1-phenyl-1*H*-pyrazolo[3,4-*d*]pyrimidin-6-yl)aniline (6h).** By use of 4-(*tert*-butoxycarbonyl-*N*-methylamino)phenylboronic acid, pinacol ester in the Suzuki−Miyaura coupling, the crude, hot reaction mixture was filtered and the residue was rinsed with hot dimethoxyethane (0.5 mL). The Boc group was removed from the resulting crude product by addition of 2 mL of TFA to the filtrate and stirring at room temperature overnight. The crude product was concentrated and used without further purification in the next step (preparation of **7**).

**Methyl [4-(4-Morpholin-4-yl-1-phenyl-1*H*-pyrazolo[3,4-*d*]pyrimidin-6- yl)phenyl]carbamate (6i).** Yield: 7 mg (0.016 $\mu$mol, 13%). LCMS: 99.1% pure, $t_R$ = 2.51 min, $m/z$ 431.2 ($[M + H]^+$).

Additional compounds (**6a**,**b**,**e**,**f**) are summarized in the Supporting Information.

***N*-Methyl-*N*-[4-(4-morpholin-4-yl-1-phenyl-1*H*-pyrazolo[3,4-*d*]pyrimidin-6-yl)phenyl]acetamide (7).** Crude *N*-methyl-4-(4-morpholino-1-phenyl-1*H*-pyrazolo[3,4-*d*]pyrimidin-6-yl)aniline (**6h**, 0.12 mmol) was treated with acetic anhydride (0.5 mL) for 2 h. The solvents were removed and the crude product was dissolved in DMSO, filtered, and purified by HPLC (TFA buffers) to give 21 mg (0.049 mmol, 41%) of the title compound. LCMS: 96% pure, $t_R$ = 2.61 min, $m/z$ 429.2 ($[M + H]^+$).

**(1-Benzylpiperidin-4-yl)hydrazine Dihydrochloride (10).** Benzoic hydrazide (27 g) was dissolved in methanol (150 mL). 1-Benzylpiperidin-4-one (**8**, 37.8 g) was added and the solution heated at 30 °C for 1 h and 60 °C for a further 2 h. The solution was then cooled to 0 °C and sodium borohydride (6.8 g) added in portions. After 2 h, the solution was evaporated and the residue was partitioned between dichloromethane and water. The organic phase was then dried with anhydrous magnesium sulfate and evaporated, leaving an oil (102 g).

The oil was dissolved in water (80 mL) containing concentrated hydrochloric acid (140 mL) (any extra organic solvent released at this stage was separated). The aqueous solution was then refluxed overnight. After the mixture was cooled to 0 °C the precipitate of benzoic acid was filtered off. Water was evaporated, anhydrous ethanol was added, and the resulting precipitate was collected by filtration and dried in high vacuum. The title compound was obtained as a white solid (32.4 g). HRMS: $m/z$ 206.164 82 ($[M + H]^+$). Exptl − calcd = −0.36 mmu. $^1$H NMR (DMSO-$d_6$) indicated a mixture of diastereomeric salts: $\delta$ 11.10 (1H, bs), 7.63 (2H, m), 7.45 (3H, m), 4.27 (2H, m), 3.37−2.89 (5H, m), 2.16−1.72 (4H, m).

**1-(1-Benzylpiperidin-4-yl)-4,6-dichloro-1*H*-pyrazolo[3,4-*d*]pyrimidine (11).** To a solution of 2,4,6-trichloropyrimidine-5-carbaldehyde (**3**, 10.0 g, 47.3 mmol) in ethanol at −78 °C was added (1-benzylpiperidin-4-yl)hydrazine dihydrochloride (13.2 g, 47.3 mmol). The mixture was stirred at −78 °C for 20 min. Triethylamine (22 mL) was added slowly over 20 min. The mixture was stirred for an additional 20 min at −78 °C, followed by stirring at 0 °C for 1 h. The mixture was concentrated in vacuo without heating. The mixture was diluted with ethyl acetate (500 mL) and saturated $NaHCO_3$ (400 mL) and filtered over Celite. The layers were shaken in a separatory funnel, and the organic phase was dried ($MgSO_4$), filtered over a silica gel plug, and rinsed with ethyl acetate. The filtrate was concentrated to give 12.5 g of a red foam (34.4 mmol, 73%). MS: $m/z$ 362.1/364.1 ($[M + H]^+$). $^1$H NMR (DMSO-$d_6$): $\delta$ 10.77 (1H, bs), 8.61 (1H, s), 7.62 (2H, m), 7.48 (3H, m), 5.07 (1H, m), 4.33 (2H, m), 3.49 (2H, d, $J$ = 12 Hz), 3.27 (2H, d, $J$ = 12 Hz), 2.53 (2H, m), 2.17 (2H, d, $J$ = 12 Hz).

**4-(1-(1-Benzylpiperidin-4-yl)-6-chloro-1*H*-pyrazolo[3,4-*d*]pyrimidin-4-yl)morpholine (12).** 1-(1-Benzylpiperidin-4-yl)-4,6-dichloro-1*H*-pyrazolo[3,4-*d*]pyrimidine (**11**) (4.5 g, 11.3 mmol) was dissolved in ethanol (35 mL) and triethylamine (1.7 mL) and stirred at room temperature for 1 h. The mixture was diluted with water (200 mL) and 10 N sodium hydroxide (2.0 mL) and extracted three times with ethyl acetate. The organics were combined and dried over sodium sulfate, filtered through Magnesol, and concentrated to an oil that crystallized upon standing. The white crystals were collected by filtration, using a minimum amount of hexanes, to give 4.1 g of (**12**) (89%). MS: $m/z$ 413.3/415.3 ($[M + H]^+$). $^1$H NMR (DMSO-$d_6$): $\delta$ 8.34 (1H, s), 7.34 (4H, d, $J$ = 4.0 Hz), 7.26 (1H, m), 4.57 (1H, m), 3.88 (4H, t, $J$ = 5.0 Hz), 3.73 (4H, t, $J$ = 4.9 Hz), 3.53 (2H, s), 2.93 (2H, m), 2.50 (4H, m), 1.82 (2H, m).

**General Procedure for Suzuki−Miyaura Coupling of 4-(1-(1-Benzylpiperidin-4-yl)-6-chloro-1*H*-pyrazolo[3,4-*d*]pyrimidin-4-yl)-morpholine (12).** 4-(1-(1-Benzylpiperidin-4-yl)-6-chloro-1*H*-pyrazolo[3,4-*d*]pyrimidin-4-yl)morpholine hydrochloride (**12**, 50 mg,

0.12 mmol) was placed in a 0.5−2 mL microwave vial. Then 0.2 mmol of a boronic acid or boronate pinacol ester was added, followed by addition of 2 mL of dimethoxyethane and 0.25 mL of a 2 M aqueous solution of sodium carbonate. Tetrakis-(triphenylphosphine)palladium(0) (14 mg, 0.1 equiv) was added, and the mixture was heated for 10−20 min at 185 °C under microwave irradiation. The mixture was concentrated, dissolved in DMSO, filtered, and purified by reversed phase HPLC (TFA buffers) to give the target compounds as TFA salts unless otherwise noted.

The following compounds were prepared according to the general procedure.

**4-[1-(1-Benzylpiperidin-4-yl)-4-morpholin-4-yl-1*H*-pyrazolo[3,4-*d*]pyrimidin-6- yl]aniline (13a).** Yield: 53 mg (90 μmol, 75%). LCMS: 100% pure, $t_R$ = 1.90 min, *m*/*z* 470.3 ([M + H]$^+$). $^1$H NMR (DMSO-$d_6$): δ 8.21 (1H, s), 8.14 (2H, d, *J* = 8.7 Hz), 7.35 (4H, m), 7.27 (1H, m), 6.61 (2H, d, *J* = 8.4 hz), 6.55 (2H, bs), 4.75 (1H, m), 3.94 (4H, m), 3.77 (4H, t, *J* = 4.4 Hz), 3.56 (2H, s), 2.96 (2H, m), 2.18 (4H, m), 1.86 (2H, m).

**{4-[1-(1-Benzylpiperidin-4-yl)-4-morpholin-4-yl-1*H*-pyrazolo-[3,4-*d*]pyrimidin-6-yl]phenyl}acetic Acid (13b).** 4-(1-(1-Benzylpiperidin-4-yl)-6-chloro-1*H*-pyrazolo[3,4-*d*]pyrimidin-4-yl)morpholine hydrochloride (**12**, 400 mg, 0.97 mmol) was placed in a 20 mL microwave vial. Phenylacetic acid−4-boronic acid (380 mg, 1.45 mmol) was added, followed by addition of 5 mL of dimethoxyethane and 1.5 mL of a 2 M aqueous solution of sodium carbonate. Tetrakis(triphenylphosphine)palladium(0) (20 mg) was added, and the mixture was heated for 15 min at 175 °C under microwave irradiation. The mixture was neutralized by addition of 1 N HCl (3 mL) and was extracted with EtOAc. The organic phase was dried ($MgSO_4$). Trituration with $Et_2O$ yielded 150 mg of the title compound as a white powder. HRMS: *m*/*z* 513.258 91 ([M + H]$^+$). Exptl − calcd = −1.96 mmu.

**Methyl {4-[1-(1-Benzylpiperidin-4-yl)-4-morpholin-4-yl-1*H*-pyrazolo[3,4-*d*]pyrimidin-6-yl]phenyl}carbamate (13c).** Yield: 21 mg (33 μmol, 28%). LCMS: 100% pure, $t_R$ = 2.05 min, *m*/*z* 528.3 ([M + H]$^+$). HRMS: *m*/*z* 528.269 89 ([M + H]$^+$). Exptl − calcd = −1.88 mmu. $^1$H NMR (DMSO-$d_6$): δ 9.88 (1H, s), 8.36 (2H, d, *J* = 9.2 Hz), 8.28 (1H, s), 7.58 (2H, d, *J* = 8.8 Hz), 7.35 (4H, m), 7.26 (1H, m), 4.79 (1H, m), 3.99 (4H, bs), 3.78 (4H, t, *J* = 4.4 Hz), 3.69 (3H, s), 3.56 (2H, s), 2.96 (2H, m), 2.20 (4H, m), 1.88 (2H, m).

**General Procedure for Formation of Ureas 16.** To commercially available 4-isocyanatophenylboronic acid, pinacol ester (49 mg, 0.2 mmol) in a microwave vial was added a solution of amine (see individual compounds for details), and the mixture was stirred for 0.5−16 h. To the resulting ureidophenylboronic acid, pinacol ester **15** were added 4-(1-(1-benzylpiperidin-4-yl)-6-chloro-1*H*-pyrazolo[3,4-*d*]pyrimidin-4-yl)morpholine hydrochloride (**12**, 50 mg, 0.12 mmol) and 0.25 mL of a 2 M aqueous solution of sodium carbonate. Tetrakis(triphenylphosphine)-palladium(0) (14 mg, 0.1 equiv) was added, and the mixture was heated for 6−10 min at 185 °C under microwave irradiation. The mixture was concentrated, dissolved in DMSO, filtered, and purified by reversed phase HPLC (TFA buffers) to give the target compound as the trifluoroacetate salt.

***N*-{4-[1-(1-Benzylpiperidin-4-yl)-4-morpholin-4-yl-1*H*-pyrazolo[3,4-*d*]pyrimidin-6-yl]phenyl}-*N*′-methylurea (16a).** An amount of 1 mL of a 2 N solution of methylamine in THF was used. Excess amine and solvent were removed under a stream of nitrogen, and the ureidophenylboronic acid, pinacol ester was dissolved in dimethoxyethane (2 mL) prior to Suzuki−Miyaura coupling. Yield: 15 mg (23 μmol, 20%). LCMS: 100% pure, $t_R$ = 1.90 min, *m*/*z* 527.3 ([M + H]$^+$).

Additional compounds (**16b**−**n**) are summarized in the Supporting Information.

**1-{4-[1-(1-Benzylpiperidin-4-yl)-4-morpholin-4-yl-1*H*-pyrazolo-[3,4-*d*]pyrimidin-6- yl]phenyl}-3-cyclopropylurea (17a).** To a solution of aniline **13a** (50 mg, 0.11 mmol) in dichloromethane was added triethylamine (26 μL) and triphosgene (18 mg, 0.06 mmol). The mixture was stirred for 15 min at room temperature and was then added to a solution of cyclopropylamine (35 μL, 0.5 mmol) in dichloromethane (1 mL). After the mixture was stirred at room temperature for 25 min, the solvents were evaporated and the crude product was dissolved in DMSO, filtered, and purified by HPLC (TFA buffers) to give the title compound as the trifluoroacetate salt. Yield: 25 mg, 0.037 mmol, 34%. LCMS: 96% pure, $t_R$ = 2.00 min, *m*/*z* 553.3 ([M + H]$^+$).

**1-{4-[1-(1-Benzylpiperidin-4-yl)-4-morpholin-4-yl-1*H*-pyrazolo-[3,4-*d*]pyrimidin-6- yl]phenyl}-3-(1*H*-imidazol-2-yl)urea (17b).** To a solution of aniline **13a** (50 mg, 0.11 mmol) in dichloromethane (1 mL) containing Huenig's base (75 μL) was added triphosgene (15 mg, 0.05 mmol). The mixture was stirred for 5 min at room temperature and was then added to a suspension of 2-aminoimidazole sulfate (106 mg, 0.4 mmol) in dichloromethane (1 mL) containing Huenig's base (75 μL). The mixture was stirred at room temperature overnight, the solvents were evaporated, and the crude product was dissolved in DMSO, filtered, and purified by HPLC (TFA buffers) to give the title compound as the trifluoroacetate salt. Yield: 5 mg, 0.007 mmol, 7%. LCMS: 100% pure, $t_R$ = 1.77 min, *m*/*z* 579.3 ([M + H]$^+$).

**2-{4-[1-(1-Benzylpiperidin-4-yl)-4-morpholin-4-yl-1*H*-pyrazolo-[3,4-*d*]pyrimidin-6-yl]phenyl}-*N*-methylacetamide (18).** {4-[1-(1-Benzylpiperidin-4-yl)-4-morpholin-4-yl-1*H*-pyrazolo[3,4-*d*]pyrimidin-6- yl]phenyl}acetic acid (**13b**, 50 mg, 0.098 mmol) was dissolved in DMF (2 mL). To the solution was added EDC (25 mg, 0.13 mmol) and HOBT (16 mg, 0.12 mmol), and the mixture was stirred for 2 h. A solution of methylamine (0.25 mL, 2 M in THF) was added, and the mixture was stirred for an additional 18 h. The mixture was purified by HPLC (TFA buffers) to give the title compound as the trifluoroacetate salt. Yield: 22 mg (34 μmol, 35%). LCMS: 100% pure, $t_R$ = 1.86 min, *m*/*z* 526.3 ([M + H]$^+$).

**4-(6-Chloro-4-morpholin-4-ylpyrazolo[3,4-*d*]pyrimidin-1-yl)piperidine-1-carboxylic Acid Methyl Ester (23a).** 1-(1-Benzylpiperidin-4-yl)-6-chloro-4-morpholin-4-yl-1*H*-pyrazolo[3,4-*d*]pyrimidine (**12**, 499 mg, 1.2 mmol) was dissolved in 0.4 mL (5.2 mmol) of methyl chloroformate and 1 mL of DCM. After 3 h at room temperature the solvents were removed under reduced pressure to give the title compound. HRMS: *m*/*z* 413.184 45 ([M + H]$^+$). Exptl − calcd = 0.89 mmu. $^1$H NMR (DMSO-$d_6$): δ 8.35 (1H, s), 4.83 (1H, m), 4.08 (2H, m), 3.89 (4H, t, *J* = 5.0 Hz), 3.74 (1H, t, *J* = 4.8 Hz), 3.72 (3H, s), 3.07 (2H, bs), 2.50 (4H, m).

**6-Chloro-4-morpholin-4-yl-1-piperidin-4-yl-1*H*-pyrazolo[3,4-*d*]pyrimidine Hydrochloride (19).** The HCl salt of 1-(1-benzylpiperidin-4-yl)-6-chloro-4-morpholin-4-yl-1*H*-pyrazolo[3,4-*d*]pyrimidine (100 mg, 0.24 mmol) was converted into the free base by extraction with an aqueous 1 N NaOH solution. Traces of moisture were removed by coevaporation with 1,2-dichloroethane (DCE). The residue was dissolved in DCE (2 mL), and 1.9 mmol (0.2 mL) of α-chloroethyl chloroformate (ACE-Cl) was added along with a small amount of $K_2CO_3$, and the mixture was stirred for 5.5 h at room temperature. The reaction was quenched by addition of MeOH, and the mixture was filtered and concentrated to dryness. The mixture was dissolved in MeOH and briefly heated to reflux. The title compound was obtained in quantitative yield by evaporation of the methanol. HRMS: *m*/*z* 323.140 09 ([M + H]$^+$). Exptl − calcd = 1.92 mmu.

**6-Chloro-4-morpholin-4-yl-1-[1-(pyridin-3-ylmethyl)piperidin-4-yl]-1*H*-pyrazolo[3,4-*d*]pyrimidine (20).** 6-Chloro-4-morpholin-4-yl-1-piperidin-4-yl-1*H*-pyrazolo[3,4-*d*]pyrimidine hydrochloride (**19**, 1.2 mmol) was suspended in THF (10 mL). 3-Pyridinecarboxaldehyde (0.19 mL, 2.0 mmol) was added, followed by addition of acetic acid (85 μL) and $NaHB(OAc)_3$ (0.47 g, 2.0 mmol). The mixture was stirred at room temperature for 30 min, diluted with dichloromethane, and washed with saturated $NaHCO_3$ and a solution of NaOH (1 N). The organic phase was dried ($MgSO_4$) and concentrated. The crude product was applied to a silica gel column and eluted with a gradient of methanol (0−8%) in ethyl acetate containing 1% triethylamine. The title compound was obtained as 249 mg of an off-white

powder (0.6 mmol, 50%). HRMS: *m*/*z* 414.183 99 ([M + H]$^+$). Exptl − calcd = 0.38 mmu. $^1$H NMR ($CDCl_3$): $\delta$ 8.57 (1H, d, $J$ = 1.2 Hz), 8.51 (1H, dd, $J$ = 1.8 Hz, 5.0 Hz), 7.90 (1H, s), 7.72 (1H, dt, $J$ = 1.8 Hz, 7.4 Hz), 7.26 (1H, m), 4.75 (1H, m), 3.97 (4H, t, $J$ = 4.4 Hz), 3.84 (4H, t, $J$ = 4.8 Hz), 3.58 (2H, s), 2.99 (2H, d, $J$ = 5.2 Hz), 2.28 (4H, m), 1.92 (2H, d, $J$ = 10.8 Hz), 1.65 (1H, s).

**4-(4-Morpholino-1-(1-(pyridin-3-ylmethyl)piperidin-4-yl)-1*H*-pyrazolo[3,4-*d*]pyrimidin-6-yl)aniline (21).** 6-Chloro-4-morpholin-4-yl-1-[1-(pyridin-3-ylmethyl)piperidin-4-yl]-1*H*-pyrazolo[3,4-*d*]pyrimidine (**20**, 2.6 g, 6.4 mmol) and 4-aminophenylboronic acid, pinacol ester (1.53 g, 7.0 mmol) were dissolved in dimethoxyethane (100 mL). A 2 M aqueous solution of $Na_2CO_3$ (13 mL) was added, and the flask was flushed with nitrogen. Tetrakis-(triphenylphosphine)palladium(0) (512 mg) was added, and the mixture was heated under reflux for 20 h. The mixture diluted with ethyl acetate and water and filtered over Celite. The organic phase was washed with saturated $NaHCO_3$ (basified with NaOH to pH 11), dried ($MgSO_4$), and concentrated. The crude product was applied to a silica gel column and eluted with a gradient of methanol (0−20%) in ethyl acetate containing 1% triethylamine to give the title compound as 2.43 g (5.16 mmol, 81%) of a yellow solid, which was used in the next step without further purification.

**Methyl (4-{4-Morpholin-4-yl-1-[1-(pyridin-3-ylmethyl)piperidin-4-yl]-1*H*- pyrazolo[3,4-*d*]pyrimidin-6-yl}phenyl)carbamate Hydrochloride (22a).** To 4-(4-morpholino-1-(1-(pyridin-3-ylmethyl)piperidin-4-yl)-1*H*-pyrazolo[3,4-*d*]pyrimidin-6-yl)aniline hydrochloride (**21**, 1100 mg, 2.33 mmol) was added dichloromethane (50 mL) and triethylamine (1.43 mL) to give a yellow solution. Triphosgene (330 mg) was added, and the mixture was stirred at ambient temperature for 5 min. Methanol was added (50 mL), and the mixture was concentrated to ∼50 mL. An additional amount of methanol (50 mL) was added, and the mixture was again concentrated to ∼50 mL. This procedure was repeated one more time. The solvents were concentrated, and the mixture was dissolved in dichloromethane and washed with a solution of 0.1 N NaOH (2×). The organic phase was dried ($MgSO_4$), filtered over Magnesol, and rinsed with dichloromethane and ethyl actetate. The organic phase was concentrated and triturated from diethyl ether to give 908 mg (1.7 mmol, 74%) of an off-white powder. An additional batch of product was obtained after concentration of the mother liquor after conversion into the free base (washed with 0.1 N NaOH) followed by column chromatography to give 260 mg of an off-white powder. The combined crops of free base product were dissolved in dichloromethane, 1.3 mL of a 4 N solution of HCl in dioxane was added, and the resulting solids were collected to give 1.081 mg (1.91 mmol, 82%) of the title compound. LCMS: 100% pure, $t_R$ = 1.91 min, *m*/*z* 529.3 ([M + H]$^+$). HRMS: *m*/*z* 529.267 93 ([M + H]$^+$). Exptl − calcd = 0.29 mmu. $^1$H NMR (DMSO-$d_6$): $\delta$ 11.47 (1H, bs), 9.89 (1H, s), 9.06 (1H, s), 8.88 (1H, d, $J$ = 4.8 Hz), 8.54 (1H, d, $J$ = 8.0 Hz), 8.40 (2H, d, $J$ = 8.8 Hz), 8.32 (1H, s), 7.89 (1H, q, $J$ = 5.2 HZ), 7.59 (2H, d, $J$ = 8.8hz), 5.08 (m, 1H), 4.53 (2H, s), 4.00 (4H, bs), 3.78 (4H, t, $J$ = 4.6 Hz), 3.69 (3H, s), 3.57 (2H, d, $J$ = 12 Hz), 3.34 (2H, m), 2.60 (2H, m), 2.16 (2H, d, $J$ = 12 Hz).

Additional compounds (**22b**−**d**) are summarized in the Supporting Information.

**Isopropyl 4-(6-Chloro-4-morpholin-4-yl-1*H*-pyrazolo[3,4-*d*]pyrimidin-1-yl)piperidine-1-carboxylate (23b).** To 6-chloro-4-morpholin-4-yl-1-piperidin-4-yl-1*H*-pyrazolo[3,4-*d*]pyrimidine dihydrochloride (**19**, 1 g, 2.5 mmol) in dichloromethane (20 mL) was added triethylamine (1 mL) and a 1.0 N solution of isopropyl chloroformate in toluene (3 mL). The mixture was stirred for 3 h at room temperature, diluted with dichloromethane, and washed with saturated $NaHCO_3$. The organic phase was dried ($MgSO_4$) and concentrated to give the title compound as 1.01 g (2.5 mmol, 99%) of an off-white solid. $^1$H NMR (DMSO-$d_6$): $\delta$ 8.35 (1H, s), 4.81 (2H, m), 4.09 (2H, m), 3.89 (4H, t, $J$ = 4.8 Hz), 3.73 (4H, t, $J$ = 4.8 Hz), 3.04 (2H, bs), 1.90 (4H, m).

***tert*-Butyl 4-(6-Chloro-4-morpholin-4-yl-1*H*-pyrazolo[3,4-*d*]pyrimidin-1-yl)piperidine-1-carboxylate (23c).** 6-Chloro-4-morpholin-4-yl-1-piperidin-4-yl-1*H*-pyrazolo[3,4-*d*]pyrimidine (**19**) (0.8 g, 2.48 mmol) was dissolved in dichloromethane (10.0 mL) with excess triethylamine. Di-*tert*-butyl dicarbonate (0.65 g, 2.97 mmol) was added, and the mixture was stirred at room temperature for 1 h. The mixture was washed twice with water, and the organic phase was dried over sodium sulfate, filtered through Magnesol, and concentrated to an oil. Trituration with ether/hexanes gave a white solid, which was collected by filtration using a minimum amount of ether/hexanes to give 0.93 g (89%) of the title compound. HRMS: *m*/*z* 423.191 72 ([M + H]$^+$). Exptl − calcd = 1.12 mmu. $^1$H NMR (DMSO-$d_6$): $\delta$ 8.35 (1H, s), 4.80 (1H, m), 4.05 (2H, d, $J$ = 9.6 Hz), 3.89 (4H, t, $J$ = 4.8 Hz), 3.74 (4H, t, $J$ = 4.8 Hz), 2.99 (2H, bs), 1.88 (4H, m), 1.425 (9H, s).

**Methyl 4-[6-(4-Aminophenyl)-4-morpholin-4-yl-1*H*-pyrazolo-[3,4-*d*]pyrimidin-1-yl]piperidine-1-carboxylate (24a).** To a solution of methyl 4-(6-chloro-4-morpholin-4-yl-1*H*-pyrazolo[3,4-*d*]pyrimidin-1- yl)piperidine-1-carboxylate (**23a**, 2.3 g, 6.0 mmol) in dimethoxyethane (26 mL) was added a 2 M aqueous solution of $Na_2CO_3$ (2.6 mL) and 4-aminophenylboronic acid, pinacol ester (1.67 g, 7.6 mmol). Tetrakis(triphenylphosphine)palladium(0) (690 mg) was added, and the mixture was heated under reflux for 16 h. The mixture was diluted with ethyl acetate and water, and the organic phase was washed with water, dried ($MgSO_4$), filtered though Magnesol, and concentrated. The resulting oil was triturated with DCM and ether to give a yellow solid. The solid was collected by filtration using a minimum amount of diethyl ether to give the title compound in a yield of 1.9 g (73%). LCMS: 98% pure, $t_R$ = 2.09 min, *m*/*z* 438.2 ([M + H]$^+$). HRMS: *m*/*z* 438.2255 ([M + H]$^+$). For [M + H]$^+$ mass error = 0.7 mDa or 1.58 ppm. $^1$H NMR (DMSO-$d_6$): $\delta$ 8.21 (1H, s), 8.14 (2H, d, $J$ = 8.4 Hz), 6.61 (2H, d, $J$ = 8.4 Hz), 5.56 (2H, bs), 4.99 (1H, m), 4.11 (2H, m), 3.96 (4H, t, $J$ = 4.6 Hz), 3.77 (4H, t, $J$ = 4.8 Hz), 3.65 (3H, s), 3.10 (2H, bs), 2.01 (2H, dq, $J$ = 4.4 Hz, $J$ = 12.4 Hz), 1.92 (2H, m).

**Isopropyl 4-[6-(4-Aminophenyl)-4-morpholin-4-yl-1*H*-pyrazolo-[3,4-*d*]pyrimidin-1-yl]piperidine-1-carboxylate (24b).** To a solution of isopropyl 4-(6-chloro-4-morpholin-4-yl-1*H*-pyrazolo[3,4-*d*]pyrimidin-1- yl)piperidine-1-carboxylate (**23b**, 2.5 mmol) in dimethoxyethane (40 mL) was added a 2 M aqueous solution of $Na_2CO_3$ (5 mL) and 4-aminophenylboronic acid, pinacol ester (613 mg, 2.8 mmol). Tetrakis(triphenylphosphine)palladium(0) (200 mg) was added, and the mixture was heated under reflux for 16 h. The mixture was diluted with ethyl acetate and water and filtered over Celite. The organic phase was washed with saturated $NaHCO_3$, dried ($MgSO_4$), and concentrated. The crude product was applied to a silica gel column and eluted with a gradient of ethyl acetate (20−80%) in hexanes to give the title compound as 632 mg (1.4 mmol, 54%) of a yellow solid. NMR indicated that the product contained a small amount of triphenylphosphinoxide. An analytically pure sample was obtained by HPLC purification of 57 mg of crude product, using TFA buffers, to give 53 mg of pure sample, used for analysis of purity and biological activity. LCMS: 93% pure, $t_R$ = 2.35 min, *m*/*z* 466.2 ([M + H]$^+$).

***tert*-Butyl 4-[6-(4-Aminophenyl)-4-morpholin-4-yl-1*H*-pyrazolo-[3,4-*d*]pyrimidin-1-yl]piperidine-1-carboxylate (24c).** To a solution of *tert*-butyl 4-(6-chloro-4-morpholin-4-yl-1*H*-pyrazolo[3,4-*d*]pyrimidin-1- yl)piperidine-1-carboxylate (**23c**, 0.9 g, 2.1 mmol) in dimethoxyethane (8.5 mL) was added a 2 M aqueous solution of $Na_2CO_3$ (2.0 mL) and 4-aminophenylboronic acid, pinacol ester (0.7 g, 3.2 mmol). Tetrakis(triphenylphosphine)palladium(0) (100 mg) was added, and the mixture was heated under reflux for 16 h. The mixture was diluted with ethyl acetate and water, and the organic phase was washed with water, dried ($MgSO_4$), filtered though Magnesol, and concentrated. The resulting oil was triturated with ether and hexanes to give a yellow solid. The solid was collected by filtration using a minimum amount of diethyl ether to give the title compound in a yield of 0.85 g (85%). HRMS: *m*/*z* 480.273 25 ([M + H]$^+$). Exptl − calcd = 1.48 mmu. $^1$H NMR (DMSO-$d_6$): $\delta$ 8.21 (1H, s), 8.14 (2H, d, $J$ = 8.8 Hz), 6.60 (2H, d, $J$ = 8.4 Hz), 5.57 (2H, bs), 4.94 (1H, m), 4.09 (2H, m),

3.96 (4H, m), 3.77 (4H, t, $J$ = 4.4 Hz), 3.02 (2H, bs), 2.02 (2H, m), 1.88 (2H, m).

**General Procedure for Formation of Ureidophenyl Compounds (25−27).** The 4-[6-(4-aminophenyl)-4-morpholin-4-yl-1*H*-pyrazolo[3,4-*d*]pyrimidin-1- yl]piperidine-1-carboxylate **24a−c** (0.12 mmol) was dissolved in dichloromethane (1 mL), and triethylamine (65 $\mu$L) was added. The resulting solution was added dropwise to a solution of triphosgene (15 mg) in dichloromethane (1 mL), and the mixture was stirred at ambient temperature for 5 min. The mixture was then added to a solution of amine (see individual compounds for details), and the mixture was stirred for 2−16 h. The solvents were concentrated, and the crude product was purified by HPLC (TFA buffers).

The following compounds were prepared according to the general procedure.

**Methyl 4-(6-(4-(3-Methylureido)phenyl)-4-morpholino-1*H*-pyrazolo[3,4-*d*]pyrimidin-1-yl)piperidine-1-carboxylate (25a).** By use of the general conditions described above, methyl 4-(6-(4-aminophenyl)-4-morpholino-1*H*-pyrazolo[3,4-*d*]pyrimidin-1-yl)piperidine-1-carboxylate (**24a**) was treated with methylamine to provide **25a**. Yield: 0.110 g, 53%, white solid. HPLC: 98% pure, $t_R$ = 11.3 min. $^1$H NMR (DMSO-$d_6$): $\delta$ 8.78 (1H, s), 8.31 (2H, d, $J$ = 8.8 Hz), 8.27 (1H, s), 7.51 (2H, d, $J$ = 8.8 Hz), 6.08 (1H, m), 5.02 (1H, m), 4.11 (2H, m), 3.99 (4H, m), 3.78 (4H, m), 3.65 (3H, s), 3.12 (2H, m), 2.66 (3H, d, $J$ = 4.4 Hz), 2.01 (2H, m), 1.93 (2H, m). HRMS: $m/z$ 495.244 92 ([M + H]$^+$ observed); $m/z$ 495.246 28 ([M + H]$^+$ calculated).

***tert*-Butyl 4-(6-(4-(3-Methylureido)phenyl)-4-morpholino-1*H*-pyrazolo[3,4-*d*]pyrimidin-1-yl)piperidine-1-carboxylate (27a). 27a** was prepared according to the general procedure, using 3.2 g of *tert*-butyl 4-[6-(4-aminophenyl)-4-morpholin-4-yl-1*H*-pyrazolo-[3,4-*d*]pyrimidin-1-yl]piperidine-1-carboxylate (**24c**), 1.0 g of triphosgene, and excess methylamine in THF (2 N). Yield: 3.2 g (84%). HRMS: $m/z$ 537.293 92 ([M + H]$^+$). Exptl − calcd = 0.69 mmu. HPLC: 99% pure, $t_R$ = 14.1 min. $^1$H NMR (DMSO-$d_6$): $\delta$ 8.77 (1H, s), 8.30 (2H, d, $J$ = 8.8 Hz), 8.26 (1H, s), 7.50 (2H, d, $J$ = 8.8 Hz), 6.06 (1H, dd, $J$ = 4.4 Hz, $J$ = 5.0 Hz), 4.97 (1H, m), 4.10 (2H, m), 3.98 (4H, m), 3.78 (4H, t, $J$ = 5.2 Hz), 3.03 (2H, m), 2.66 (3H, d, $J$ = 4.4 Hz), 2.04 (2H, dq, $J$ = 3.6 Hz, $J$ = 11.6 Hz), 1.90 (2H, d, $J$ = 9.2 Hz), 1.45 (9H, s).

Additional compounds (**25b−f**, **26b**,**c**, **27b**,**c**) are summarized in the Supporting Information.

**1-Methyl-3-(4-(4-morpholino-1-(piperidin-4-yl)-1*H*-pyrazolo[3,4-*d*]pyrimidin-6-yl)phenyl)urea (28).** To a solution of *tert*-butyl 4-(6-(4-(3-methylureido)phenyl)-4-morpholino-1*H*-pyrazolo[3,4-*d*]pyrimidin-1-yl)piperidine-1-carboxylate (**27a**) (3.2 g 5.97 mmol) in dichloromethane (40 mL) was added trifluoroacetic acid (excess), and the mixture was stirred at room temperature for 2 h and then concentrated. The residue was treated with 2 N HCl and extracted 2 times with dichloromethane. The aqueous phase was basified with sodium hydroxide and extracted 4 times with ethyl acetate. The combined organics were dried with sodium sulfate, filtered, and concentrated to a white solid. The solid was dissolved in acetonitrile, and a solution of HCl in MeOH was added to precipitate a white solid. The solid was collected by filtration and washed with acetonitrile to afford 2.6 g of the title compound (94%). LCMS: 99% pure, $t_R$ = 1.69 min, $m/z$ 437.2 ([M + H]$^+$). HRMS: $m/z$ 437.240 38 ([M + H]$^+$). Exptl − calcd = −0.42 mmu. $^1$H NMR (DMSO-$d_6$): $\delta$ 8.82 (1H, s), 8.34 (2H, d, $J$ = 8.8 Hz), 8.31 (1H, s), 7.52 (2H, d, $J$ = 8.8 Hz), 6.11 (1H, d, $J$ = 4.8 Hz), 5.12 (1H, m), 4.00 (4H, m), 3.78 (4H, t, $J$ = 4.8 Hz), 3.47 (2H, d, $J$ = 12.8 Hz), 3.24 (2H, q, $J$ = 11.2 Hz), 2.66 (3H, d, $J$ = 4.4 Hz), 2.26 (2H, q, $J$ = 13.2 Hz), 2.12 (2H, d, $J$ = 11.6 Hz).

**Methyl 4-(6-(4-(3-Methylureido)phenyl)-4-morpholino-1*H*-pyrazolo[3,4-*d*]pyrimidin-1-yl)piperidine-1-carboxylate (25a).** To a solution of 1-methyl-3-[4-(4-morpholin-4-yl-1-piperidin-4-yl-1*H*-pyrazolo[3,4-*d*]pyrimidin-6-yl)phenyl]urea (**28**, 200 mg, 0.42 mmol) in dichloromethane (4.0 mL) and triethylamine (excess) was added methyl chloroformate (0.040 mL), and the mixture was stirred at room temperature for 1 h. The mixture was washed 3 times with water, and the organics were combined and dried over sodium sulfate. The mixture was filtered over Magnesol and eluted with ethyl acetate. The filtrate was concentrated to a crude solid. The solid was recrystallized 2 times from acetonitrile to give 64 mg (31%) of the title compound. The thus obtained compound was identical to **25a** obtained according to Scheme 5. LCMS: 92% pure, $t_R$ = 2.18 min, $m/z$ 495.2 ([M + H]$^+$). $^1$H NMR (DMSO-$d_6$): $\delta$ 8.78 (1H, s), 8.31 (2H, d, $J$ = 8.8 Hz), 8.27 (1H, s), 7.51 (2H, d, $J$ = 8.8 Hz), 6.08 (1H, m), 5.02 (1H, m), 4.11 (2H, m), 3.99 (4H, m), 3.78 (4H, m), 3.65 (3H, s), 3.12 (2H, m), 2.66 (3H, d, $J$ = 4.4 Hz), 2.01 (2H, m), 1.93 (2H, m).

**Isopropyl 4-(6-(4-(3-Methylureido)phenyl)-4-morpholino-1*H*-pyrazolo[3,4-*d*]pyrimidin-1-yl)piperidine-1-carboxylate (26a).** To a solution of 1-methyl-3-[4-(4-morpholin-4-yl-1-piperidin-4-yl-1*H*-pyrazolo[3,4-*d*]pyrimidin-6- yl)phenyl]urea (**28**, 40 mg, 0.08 mmol) in dichloromethane (1.0 mL) and triethylamine (excess) was added isopropyl chloroformate (excess), and the mixture was stirred at room temperature for 1 h. The crude product was purified by HPLC using TFA buffers to give 13.8 mg (31%). LCMS: 100% pure, $t_R$ = 2.34 min, $m/z$ 523.3 ([M + H]$^+$).

**Methyl 4-(4-Morpholino-6-(4-(3-(4-(2-(pyrrolidin-1-yl)ethyl)-phenyl)ureido)phenyl)-1*H*-pyrazolo[3,4-*d*]pyrimidin-1-yl)piperidine-1-carboxylate (25g).** A solution of methyl 4-(6-(4-(3-(4-(2-hydroxyethyl)phenyl)ureido)phenyl)-4-morpholino-1*H*-pyrazolo[3,4-*d*]pyrimidin-1-yl)piperidine-1-carboxylate (**25f**) (0.060 g, 0.099 mmol) in methylene chloride (1 mL) was prepared. Triethylamine (0.041 mL, 0.23 mmol) was added, followed by *p*-toluenesulfonyl chloride (0.019 g, 0.099 mmol), and the solution was stirred at room temperature for 3 h. The solution was then diluted with methylene chloride, washed with saturated sodium bicarbonate, brine, dried ($Na_2SO_4$), decanted, and concentrated under reduced pressure. The crude tosylate (0.049 mmol) was dissolved in methylene chloride (1 mL), and pyrrolidine (0.038 mL, 0.450 mmol) was added. The solution was stirred at room temperature for 14 h. Solvent was removed under reduced pressure. Purification by HPLC provided **25g**. Yield: 0.010 g, 34%, white solid. LCMS: 100% pure, $t_R$ = 2.05 min, $m/z$ 654.3 ([M + H]$^+$).

Additional compounds (**25h**,**i**) are summarized in the Supporting Information.

**Acknowledgment.** The authors thank Dr. Joseph Marini and Angela Bretz for nude mouse microsome assays, Dr. Li Di and Susan Li for human microsome assays, Rob Mahoney and Kenny Kim for in vivo biomarker inhibition assays, Dr. Richard Harrison, Dr. Ann Aulabaugh, Jenny Togias, and Kenneth Roberts for kinase panel assays, and Dr. Frank Loganzo, Cheng-Chung Tsao, and William Hu for ATR assays.

**Supporting Information Available:** Experimental details for compounds **6a**,**b**,**e**,**f**, **16b−n**, **22b−d**, **25b−f**,**h**,**i**, **26b**,**c**, **27b**,**c**; synthesis and SAR of additional analogues; activity against a broad panel of tumor cell lines for **13o**, **18a**, **24a**, and **24c**; kinase panel selectivity data for **24a**, **24c**, and **29a**. This material is available free of charge via the Internet at http://pubs.acs.org.

## References

(1) Guertin, D. A.; Sabatini, D. M. Defining the role of mTOR in cancer. *Cancer Cell* **2007**, *12*, 9–22.
(2) Chiang, G. G.; Abraham, R. T. Targeting the mTOR signaling network in cancer. *Trends Mol. Med.* **2007**, *13*, 433–442.
(3) Yuan, T. L.; Cantley, L. C. PI3K pathway alterations in cancer: variations on a theme. *Oncogene* **2008**, *27*, 5497–5510.
(4) Verheijen, J. C.; Zask, A. Phosphatidylinositol 3-kinase (PI3K) inhibitors as anticancer drugs. *Drugs Future* **2007**, *32*, 537–547.
(5) Verheijen, J. C.; Yu, K.; Zask, A. mTOR Inhibitors in Oncology. *Annu. Rep. Med. Chem.* **2008**, *43*, 189–202.
(6) Sarbassov, D. D.; Ali, S. m.; Kim, D. H.; Guertin, D. A.; Latek, R. R.; Erdjument-Bromage, H.; Tempst, P.; Sabatini, D. M. Rictor, a

novel binding partnet of mTOR, defines a rapamycin-insensitive and raptor-independent pathway that regulates the cytoskeleton. *Curr. Biol.* **2004**, *14*, 1296–1302.
(7) Sarbassov, D. D.; Guertin, D. A.; Ali, S.m.; Sabatini, D. M. Phosphorylation and regulation of Akt/PKB by the Rictor-mTOR complex. *Science* **2005**, *307*, 1098–1101.
(8) Carracedo, A; Pandolfi, P. P. The PTEN-PI3K pathway: of feedbacks and cross-talks. *Oncogene* **2008**, *27*, 5527–5541.
(9) Choo, A. Y.; Yoon, S. O.; Kim, S. G.; Roux, P. P.; Blenis, J. Rapamycin differentially inhibits S6Ks and 4E-BP1 to mediate cell-type-specific repression of mRNA translation. *Proc. Natl. Acad. Sci. U.S.A.* **2008**, *105*, 17414–17419.
(10) Guertin, D. A.; Sabatini, D. M. The Pharmacology of mTOR Inhibition. *Sci. Signaling* **2009**, *2*, 1–6.
(11) Folkes, A. J.; Ahmadi, K.; Alderton, W. K.; Alix, S.; Baker, S. J.; Box, G.; Chuckowree, I. S.; Clarke, P. A.; Depledge, P.; Eccles, S. A.; Friedman, L. S.; Hayes, A.; Hancox, T. C.; Kugendradas, A.; Lensun, L.; Moore, P.; Olivero, A. G.; Pang, J.; Patel, S.; Pergl-Wilson, G. H.; Raynaud, F. I.; Robson, A.; Saghir, N.; Salphati, L.; Sohal, S.; Ultsch, M. H.; Valenti, M.; Wallweber, H. J. A.; Wan, N. C.; Wiesmann, C.; Workman, P.; Zhyvoloup, A.; Zvelebil, M. J.; Shuttleworth, S. J. The identification of 2-(1*H*-indazol-4-yl)-6-(4-methanesulfonyl-piperazin-1-ylmethyl)-4-morpholin-4-yl-thieno[3,2-*d*]pyrimidine (GDC-0941) as a potent, selective, orally bioavailable inhibitor of class I PI3 kinase for the treatment of cancer. *J. Med. Chem.* **2008**, *51*, 5522–5532.
(12) Maira, S.-M.; Stauffer, F.; Brueggen, J.; Furet, P.; Schnell, C.; Fritsch, C.; Brachmann, S.; Chene, P.; De Pover, A.; Schoemaker, K.; Fabbro, D.; Gabriel, D.; Simonen, M.; Murphy, L.; Finan, P.; Sellers, W.; Garcia-Echeverria, C. Identification and characterization of NVP-BEZ235, a new orally available dual phosphatidylinositol 3-kinase/mammalian target of rapamycin inhibitor with potent in vivo antitumor activity. *Mol. Cancer Ther.* **2008**, *7*, 1851–1863.
(13) Knight, Z. A.; Gonzalez, B.; Feldman, M. E.; Zunder, E. R.; Goldenberg, D. D.; Williams, O.; Loewith, R.; Stokoe, D.; Balla, A.; Toth, B.; Balla, T.; Weiss, W. A.; Williams, R. L.; Shokat, K.M. A Pharmacological map of the PI3-K family defines a role for p110α in insulin signaling. *Cell* **2006**, *125*, 733–747.
(14) Feldman, M. E.; Apsel, B.; Uotila, A.; Loewith, R.; Knight, Z. A.; Ruggero, D.; Shokat, K. M. Active-site inhibitors of mTOR target rapamycin-resistant outputs of mTORC1 and mTORC2. *PLoS Biol.* **2009**, *7*, 371–383.
(15) Thoreen, C. C.; Kang, S. A.; Chang, J. W.; Liu, Q.; Zhang, J.; Gao, Y.; Reichling, L. J.; Sim, T.; Sabatini, D. M.; Gray, N. S. An ATP-competitive mammalian target of rapamycin inhibitor reveals rapamycin-resistant functions of mTORC1. *J. Biol. Chem.* **2009**, *284*, 8023–8032.
(16) García-Martínez, J. M.; Moran, J.; Clarke, R. G.; Gray, A.; Cosulich, S. C.; Chresta, C. M.; Alessi, D. R. Ku-0063794 is a specific inhibitor of the mammalian target of rapamycin (mTOR). *Biochem. J.* **2009**, *421*, 29–42.
(17) Menear, K. A.; Gomez, S.; Malagu, K.; Bailey, C.; Blackburn, K.; Cockroft, X.-L.; Ewen, S.; Fundo, A.; Le Gall, A.; Hermann, G.; Sebastian, L.; Sunose, M.; Presnot, T.; Torode, E.; Hickson, I.; Martin, N. M. B.; Smith, G. C. M.; Pike, K. G. Identification and optimization of novel and selective small molecular weight kinase inhibitors of mTOR. *Bioorg. Med. Chem. Lett.* **2009**, *19*, 5898–5901.
(18) Malagu, K.; Duggan, H.; Menear, K.; Hummersone, M.; Gomez, S.; Bailey, C.; Edwards, P.; Drzewiecki, J.; Leroux, F.; Quesada, M. J.; Hermann, G.; Maine, S.; Molyneaux, C.-A.; Le Gall, A.; Pullen, J.; Hickson, I.; Smith, L.; Maguire, S.; Martin, N.; Smith, G.; Pass, M. The discovery and optimization of pyrido[2,3-*d*]pyrimidine-2,4-diamines as potent and selective inhibitors of mTOR kinase. *Bioorg. Med. Chem. Lett.* **2009**, *19*, 5950–5953.
(19) Zask, A.; Verheijen, J.; Kaplan, J.; Curran, K.; Richard, D.; Brooijmans, N.; Lucas, J.; Toral-Barza, L.; Zhang, W.-G.; Hollander, I.; Gibbons, J.; Abraham, R.; Ayral-Kaloustian, S.; Mansour, T.; Yu, K. Design and synthesis of potent and selective ATP competitive inhibitors of the mammalian target of rapamycin. *J. Med. Chem.* **2009**, *52*, 5013–5016.
(20) Nowak, P.; Brooijmans, N.; Cole, D. C.; Curran, K. J.; Ellingboe, J.; Gibbons, J. J.; Hu, Y.; Hollander, I.; Kaplan, J.; Malwitz, D. J.; Toral-Barza, L.; Verheijen, J.; Zask, A.; Zhang, W.-G.; Yu, K. Discovery of potent and selective inhibitors of the mammalian target of rapamycin (mTOR) kinase. *J. Med. Chem.* DOI: 10.1021/jm9012642.
(21) Yu, Y.; Toral-Barza, L.; Shi, C.; Zhang, W.-G.; Lucas, J.; Shor, B.; Kim, J.; Verheijen, J.; Curran, K.; Malwitz, D. J.; Cole, D. C.; Ellingboe, J.; Ayral-Kaloustian, S.; Mansour, T. S.; Gibbons, J. J.; Abraham, R. T.; Nowak, P.; Zask, A. Biochemical, cellular and in vivo activity of novel ATP-competitive and selective inhibitors of the mammalian target of rapamycin. *Cancer Res.* **2009**, *69*, 6232–6240.
(22) Fenniri, H.; Mathivanan, P.; Vidale, K. L.; Sherman, D. M.; Hallenga, K.; Wood, K. V.; Stowell, J. G. Helical rosette nanotubes: design, self-assembly, and characterization. *J. Am. Chem. Soc.* **2001**, *123*, 3854–3855.
(23) Toral-Barza, L.; Zhang, W. G.; Lamison, C.; Larocque, J.; Gibbons, J.; Yu, K. Characterization of the cloned full-length and a truncated human target of rapamycin: activity, specificity, and enzyme inhibition as studied by a high capacity assay. *Biochem. Biophys. Res. Commun.* **2005**, *332*, 304–310.
(24) Zask, A.; Kaplan, J.; Toral-Barza, L.; Hollander, I.; Young, M.; Tischler, M.; Gaydos, C.; Cinque, M.; Lucas, J.; Yu, K. Synthesis and structure−activity relationship of ring-opened 17-hydroxywortmannins: potent phosphoinositide 3-kinase inhibitors with improved properties and anticancer efficacy. *J. Med. Chem.* **2008**, *51*, 1319–1323.
(25) Yu, K.; Toral-Barza, L.; Discafani, C.; Zhang, W. G.; Skotnicki, J.; Frost, P.; Gibbons, J. mTOR, a novel target in breast cancer: the effect of CCI-779, an mTOR inhibitor, in preclinical models of breast cancer. *Endocr.-Relat. Cancer* **2001**, *8*, 249–258.
(26) Yu, K.; Lucas, J.; Zhu, T.; Zask, A.; Gaydos, C.; Toral-Barza, L.; Gu, J.; Li, F.; Chaudhary, I.; Cai, P.; Lotvin, J.; Petersen, R.; Ruppen, M.; Fawzi, M.; Ayral-Kaloustian, S.; Skotnicki, J.; Mansour, T.; Frost, P.; Gibbons, J. PWT-458, a novel pegylated-17-hydroxywortmannin, inhibits phosphatidylinositol 3-kinase signaling and suppresses growth of solid tumors. *Cancer Biol. Ther.* **2005**, *5*, 538–545.
(27) Tsou, H.-R.; Liu, X.; Birnberg, G.; Kaplan, J.; Otteng, M.; Tran, T.; Kutterer, K.; Tang, Z.; Suayan, R.; Zask, A.; Ravi, M.; Bretz, A.; Grillo, M.; McGinnis, J. P.; Rabindran, S. K.; Ayral-Kaloustian, S.; Mansour, T. S. Discovery of 4-(benzylaminomethylene)isoquinoline-1,3-(2*H*,4*H*)-diones and 4-[(pyridylmethyl)-aminomethylene]isoquinoline-1,3-(2*H*,4*H*)-diones as potent and selective inhibitors of the cyclin-dependent kinase 4. *J. Med. Chem.* **2009**, *52*, 2289–2310.